DRAG REDUCTION IN AQUEOUS FLOW SYSTEMS

BY

ZBIGNIEW, JAN CZABAN, B.ENG.

A Thesis

Submitted to the Faculty of Graduate Studies

in Partial Fulfilment of the Requirements

for the Degree

Master of Engineering

McMaster University

February 1974

MASTER OF ENGINEERING (1974) McMASTER UNIVERSITY
(Mechanical Engineering) (Hamilton, Ontario)

TITLE: "Drag Reduction in Aqueous Flow Systems"

AUTHOR: Zbigniew, Jan Czaban, B.Eng.
(McMaster University)

SUPERVISOR: Dr. B. Latto

NUMBER OF PAGES: v,69

SCOPE AND CONTENTS:

This thesis presents an experimental study of the drag reduction effects obtained from injecting additive solutions into a turbulent boundary layer developing over a flat plate submerged in water. Both direct injection, from a reservoir through a slit adjacent to the flat plate test section, and ablative coating methods of introducing the additive were studied.

Drag reduction data were obtained for polymeric and micelle materials. The test conditions included varying the free stream velocity over the plate from 1.9 to 5.4 fps and injecting the additives in concentrations of up to 2000 wppm at rates up to 50 ml/sec over the test section of the flat plate.

It was found that although optimal injection rates exist, drag reduction seems to be a function of how much additive is present in the flow over a test surface and not how it was delivered there. It was also found that ablative coatings of the type used for these experiments seem to have a long life expectancy and produce noticeable drag reduction.

ACKNOWLEDGEMENTS

The author wishes to thank Dr. B. Latto, under whose guidance this research was carried out, for his understanding, encouragement and assistance during the course of this program.

Samples of Reten 423, supplied by Hercules Inc. Wilmington, Delaware, free of charge, are gratefully acknowledged.

This research was supported financially in part by the National Research Council and by the Defence Research Board of Canada

TABLE OF CONTENTS

NOMENCLATURE

SYMBOL	DESCRIPTON	UNITS
C_f	Local coefficient of skin friction $= \frac{\tau_o}{\frac{1}{2}\rho U^2}$	
δ	Boundary layer thickness	in or ft
δ_θ	Momentum thickness	in or ft
D	Measured drag on test section of flat plate	(oz/ft^2)
ΔD	Change in measure drag over test section due to additive employment	(oz/ft^2)
$\Delta D/D$	Percentage drag reduction	%
F_{tot}	Total drag force on a flat plate	(lb_f/ft^2)
g	Gravitational constant	$32.2\left(\frac{lb_m\text{-}ft}{lb_f\text{-}sec^2}\right)$
H_1	Height of fluid level in rheometer reservoir above bottom of capillary	ft
Hz	Display on velocity probe meter	hertz
k	Capillary inlet losses factor	
L	Length, measured from leading edge of flat plate	ft
μ	Absolute viscosity	$lb\text{-}sec/ft^2$
ν	Kinematic viscosity	ft^2/sec
P_1	Pressure in rheometer reservoir	psi
P_2	Pressure at bottom of rheometer capillary	psi
Q_{in}	Total additive injection rate	gm polymer/sec
Q_{bl}	Boundary layer flowrate	cfs
ρ	Density	lb_m/ft^3
Re_L	Reynolds number $= \left(\frac{LU_\infty}{\nu}\right)$	

SYMBOL	DESCRIPTION	UNITS
Re_x	Reynolds number $= (\frac{xU}{\nu})$	
$(Re_x)_{cr}$	Critical Reynolds number, below which only laminar flow exists	
τ_o	Wall shear stress $= (\frac{\partial u}{\partial y})_{y_o}$	lb_f/ft^2
u	Longitudinal velocity	fps
U_∞	Free stream velocity	fps
V_1	Velocity of moving fluid level in rheometer reservoir	fps
V_2	Velocity of moving fluid level in rheometer capillary	fps
w	Width of test section	in or ft
wppm	Abbreviation for weight parts of additive per one million weight parts of solvent	
x	Distance along flat plate measured from leading edge	ft
y	Distance normal to the plate surface	ft

CHAPTER I

INTRODUCTION:

The production and application of synthetic and organic polymers has expanded considerably. That trace additions of high polymers in solution reduce drag in certain concentrations has been well established. However, the behaviour of polymer solutions on flows other than internal pipe flows has not yet been fully dealt with. At the time this research was instigated, there were approximately eight papers available on drag reduction over flat plates most of which tended to be descriptive or qualitative. Semi-empiric relationships are difficult to establish due to differring experimental techniques.

Few correlations are available that could possibly be used for actual design criteria. Ultimate possible drag reduction predictions, based upon internal flow data, are available. However, the ultimate drag predictions are seldom met and not all of the new polymers have been investigated.

Some of the main hinderances to a better understanding of the flow phenomena involved and the difficulty in obtaining universal correlations for dilute polymer flows are, for example, the extremely low concentration of the additives required (usually less than 40 weight parts per million), the complicated nature of the additive molecular structure or molecular weight distribution, and the extreme sensi-

tivity of these fluids to mechanical, chemical and bacterial degradation, as well as specific type differences which arise from having a large number of additives that form these fluids.

The concentration of polymer additive required for drag reduction or other flow control purposes is so low that for all practical purposes a solution will retain the thermodynamic and physical properties of the solvent. Thus, even though some polymers are decidedly non-Newtonian at very low concentrations, most of the solutions are Newtonian in their general behaviour but are seen to contain long chains of molecules which appear to alter some of the fluid flow mechanisms.

In the majority of external flows it is obvious that, for economical application, the additive should be kept near the wall. Boundary layer injections and ablative coatings permit such an application although the most efficient methods for their employment remain uncertain. Injection velocity and angle, pulsing of injection and injection concentration must all be considered for drag reduction efficiency.

This thesis is one of a continuing set of investigations being conducted in this laboratory, the present program of which, is to obtain empiric and theoretical data on high molecular weight polymer addition flows as well as dilute suspension flows and alternative solutions, in order to establish general relationships for determining

skin friction coefficient variation, overall drag reduction and turbulent diffusion characteristics for external and internal flows. Experimental data were obtained in a systematic investigation of additive injection into the boundar layer over a flat plate. These data were used to further the abovementioned relationships.

Ablative coatings were manufactured and investigated for drag reducing characterisitics, diffusion rates and life expectancy as a possible economic substitute for drag reduction by injection.

Viscosity data were obtained for various concentrations of Reten 423, one of the polyacrylamides used in this investigation, to establish its physical behavior.

CHAPTER II

LITERATURE SURVEY:

A brief survey of the more pertinent research on external flows over flat plates will be presented here. For a more comprehensive review of drag reduction using high molecular weight additives it is suggested that reference be made to recently published review papers by Hoyt(1) and Gadd(2). Furthermore, summaries of world literature on this topic are prepared by the U.S. Naval Ship Research and Development Center under the title "Progress in Frictional Drag Reduction," annually.

Most analytical studies of polymer solution flows over flat plates have been based upon the similarities between pipe flow and flat plate flow, as internal flow data generally is more readily available. Granville(3) and Giles(4) exploited these similarities and obtained a relationship predicting the minimum skin friction obtainable on a flat plate by optimum employment of drag-reducing polymers. The Giles(4) result is expressed as,

$$C_f = 0.315(Re_x)^{-0.362} \qquad (2.1)$$

These methods indicate maximum possible drag reductions of 80 percent or more at Reynolds numbers greater than 10^9. It must be realized however, that a uniform concentration of polymer is ensured within a pipe and that most data originating from internal

flows is not length but diameter Reynolds number dependent. Injections of polymer into developing boundary layers over flat plates do not assume uniform concentrations therein and are found to diffuse into the free stream, thus decreasing in concentration with distance from their point of introduction, Latto(5).

Most of the flat plate drag measurement experiments used either towing tanks Emerson(6), Levy and Davis(7), or recirculating open channels Latto et al(8), White(9). These investigations employed uniform concentrations of polymer as the free stream medium and although the maximum drag reduction predicted by Giles was approached it was never attained. Generally, maximal reduction effects were noticed at concentrations of 15 weight parts per million (wppm) with additives having molecular weights of the order of 10^6. Increasing the Reynolds number was found to increase the effectiveness of the additives.

The most important series of experiments for the purpose of this dissertation and for practical applications is that of polymer injection into the boundary layer over a flat plate. Love (10) ejected polymer from slots on each side of the leading edge of a 1.5 ft long plate situated in a recirculating water channel. A wake survey estimated the friction reduction on the plate. A 50 percent drag reduction was obtained at low flow rates using a 50 wppm average injection concentration.

A large amount of data were published by Tulin and Wu(14)

on ejection quantities, polymer concentrations, and slot widths for a 10 by 21 inch flat plate at a free stream velocity of 8 fps. They found that the optimum discharge concentration was 100 wppm, a narrow slot was best and that the fluid should be ejected at a flow rate near that of the viscous sublayer.

Kowalski (11) investigated drag reduction on a 19 foot boat with the aim of reducing the quantities of polymer required. The turbulence was observed to change from small amplitude to larger amplitude turbulent velocity fluctuations, with the introduction of polymers. He suggested that the change in turbulent viscous drag was due to the high frequency energy dissipating eddies shifting to lower frequencies thus conserving energy. He also noted that an injection of one second duration followed by a ten second pause, was almost as effective in reducing drag as was that of a continuous injection. He also reported finding that injecting parallel to the surface was about ten times as effective as injecting normal to the wall.

Kilian(12) coated a smooth plexiglass plate with 15000 wppm solution of Polyox WSR-301. The solution dried on the surface and the whole plate was towed at $Re=10^6$. Although the polymer washed off after 25 seconds the flat plate resistance was lowered by 10 percent.

Tagori and Kim (13), using a porous plate indicated

the drag reduction effect may be kept very efficient if the polymer is kept close to the wall.

Astarita and Nicodemo(15) recognized that significant errors could occur in measurement surveys of velocity distributions when polymers were present. Total pressure tube errors in polymer solutions were attributed to the following points; normal stress term influences, the time average of the fluctuating stresses are not simply related to the time average of the velocity distributions, the boundary-layer thickness on the pressure probe may be large compared with the probe size, and possible entanglement of the large molecules around the probe itself. A larger instrument, in the order of 3/8 inch diameter, was found to have negligible error in various concentrations of polymer but a corresponding loss in accuracy of velocity profile measurement due to averaging over a larger probe area was encounterred. It is recommended that pitot-tube type instruments be used only in situations where precise calibrations are possible.

Polymers also affect the flow and heat transfer characteristics of cylinders, thus hot wire type probes show significant error when used in polymer solutions. Hot film anemometers show more promise but are still affected by molecular entanglements and differing heat transfer rates.

There is very little information, in the literature, about the diffusion of polymers in aqueous solutions, especially with regard to injection from slits or point sources. Information on the effectiveness and methods of producing ablative coatings is virtually non-existent. Comparing existing data is very difficult because flow conditions vary markedly between different researchers and no data exists for the newer much heavier molecular weight additives.

It has been attempted wherever possible to establish the results of these experimental data such that their effects could be traceable to a particular amount of additive present in a defineable flow situation. A number of additive types were used, including one of a molecular weight of the order of 10^8, such that their effects could be compared directly.

CHAPTER III

EXPERIMENTAL APPARATUS:

3.1 The Tilting Flume

The free stream conditions were created within a 30 foot long tilting flume with a cross section of 12.2 inch width and approximate 18 inch depth. A large tank supplied a constant pressure head to the flume. It was continuously filled by a 10 Hp 1400 USGPM pump drawing from a 2000 cubic foot reservoir into which the flume discharged.

The flume walls are of glass and permit visual observations. Two rails along the top of the flume provide an accurate datum for measuring instrumentation. It is possible to control the flow by three mechanisms. The inlet head is controlled by an 8 inch gate valve located directly below the supply tank, the flume discharge is controlled by a tail gate, and additional head may be provided by tilting the flume itself.

The system had to be modified as it only produced velocities of $2\frac{1}{2}$ fps. Reynolds numbers of 10^7 were required, but the limiting factor turned out to be the pump and Reynolds numbers of 5×10^6 could only be achieved. Higher Reynolds numbers could be obtained by decreasing the height of the flow which produced severely skewed velocity profiles. The modifications included altering the flume catch basin to prevent flooding, baffling the flume so as to reduce

its cross section thus reducing the required mass flow, providing a vortex degenerator in the downpipe from the header tank to destroy the large vorticies which effectively restricted higher mass flowrates, and tilting the entire flume to provide additional head.

3.2 The Flat Plate

The flat plate, shown in Figure 3.1 was designed for this experiment such that a fully developed turbulent boundary layer would be formed over the entire working section.

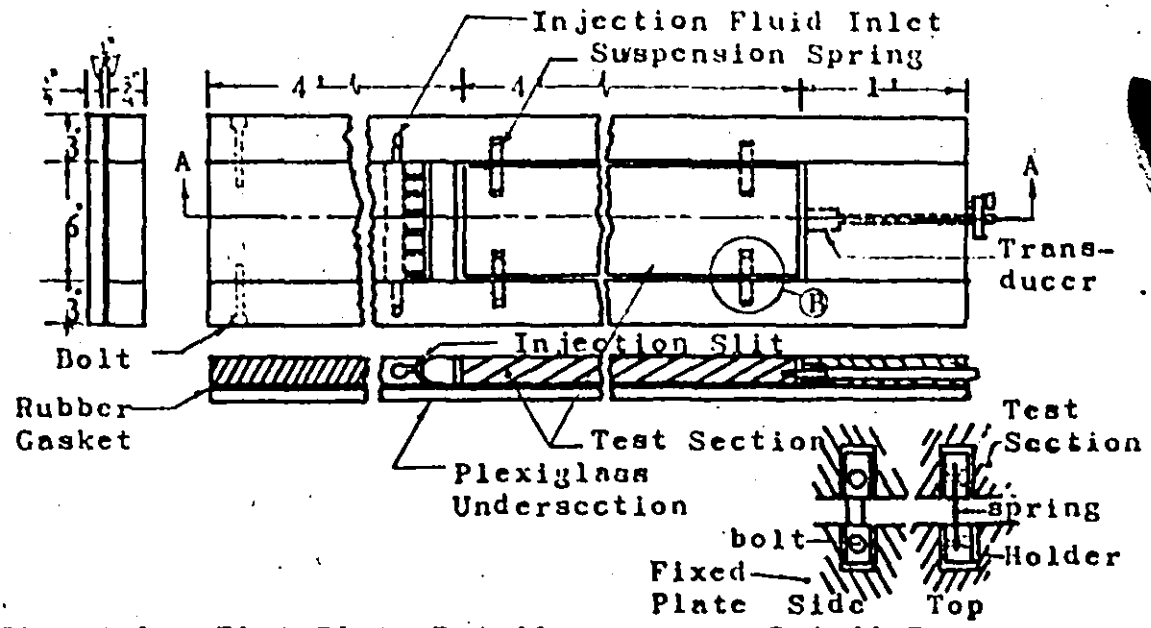

Figure 3.1 Flat Plate Detail

The plate is made of 3/4 inch stock aluminum, 1 foot wide and 9 feet long. There is a 6 inch wide working section 4 feet in length mounted flush with the frame plate. The working section is suspended from the frame by four .005 inch thick stainless steel springs which prevent vertical movement of the test section, yet allow it to

move longitudinally against their combined spring rate. The test section is flat to within .002 inches and has water tight air pockets within it which provide a neutral bouyancy in water and reduce the total weight on the spring mechanism. The test section is connected to a Schaevitz linear variable differential transformer mounted so as to allow zero adjustment. A .005 inch, 6 inch wide injection slit, located just upstream of the test section allows additive injections to be made parallel to the plate surface. Tubing connects the slit to the injection cylinder.

The underside of the frame section of the plate is attached to a 1/4 inch sheet of plexiglass using a 1/8 inch rubber gasket which prevents the test section from touching the plexiglass and forms a water tight seal around the plate perimeter thus preventing drag on the underside of the test section.

The whole assembly, as shown in Figure 3.2, is located such that the leading edge of the flat plate is 12 feet downstream of the flume inlet downpipe. It is supported by two 9 foot lengths of $1\frac{1}{2}$ by $\frac{1}{4}$ inch aluminum strip which rest on the flume floor and allow flow under the plate.

Thus the boundary layer which is developing along the flume floor passes underneath the plate and a reasonably uniform flow field is supplied to the leading edge of the plate.

The resultant flow impinges upon a blunt 1 1/8 inch leading edge whereupon it is subjected to 8 inches of number 120 waterproof sandpaper, these being turbulence tripping mechanisms to ensure the flow field becoming turbulent at the lowest possible Reynolds number of 300,000. Figure 5.1 confirms that in fact turbulence was obtained at this Reynolds number. Thus turbulent flow is obtained over the test section, which is located 4 feet downstream of the plates leading edge, even at free stream velocities of less than 2 fps.

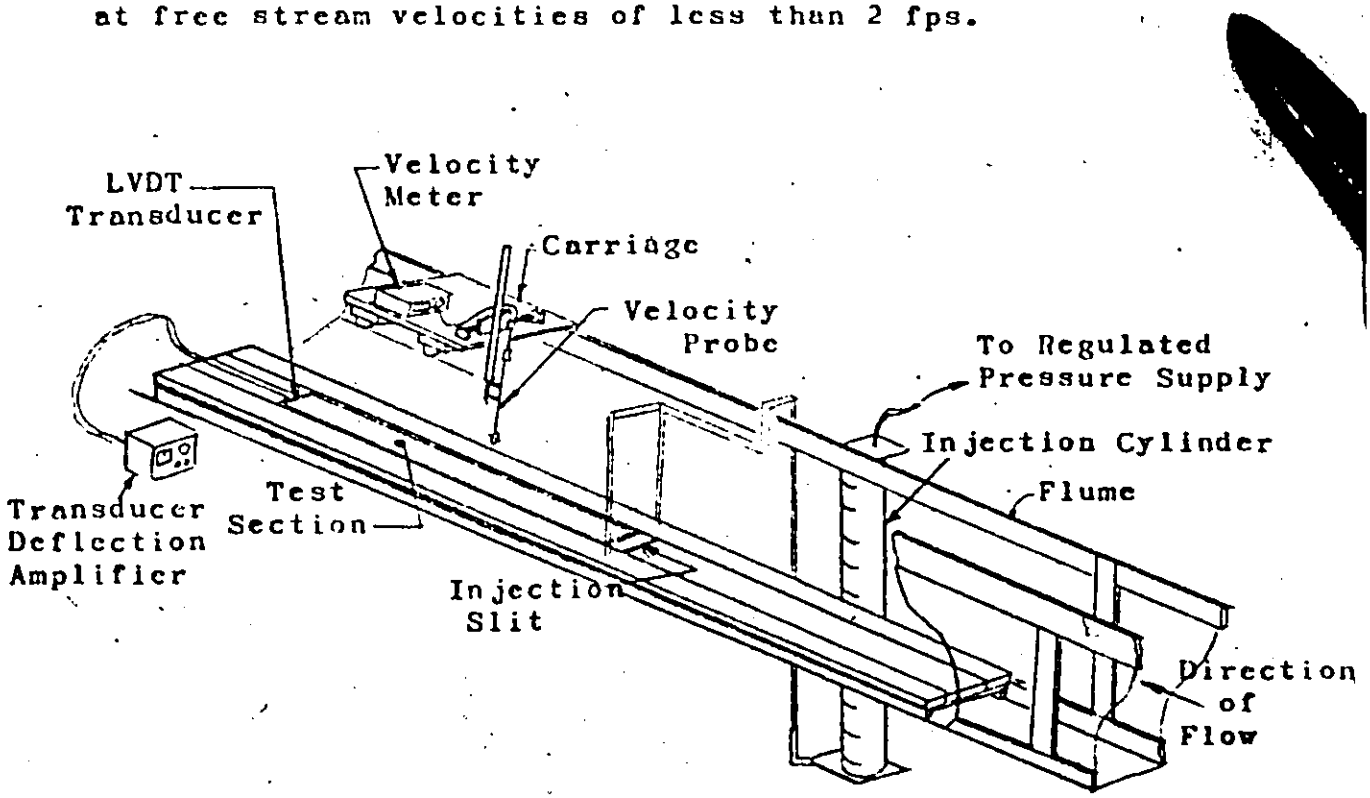

Figure 3.2 The Flat Plate and Auxiliary Equipment.

3.3 Auxiliary Instrumentation

The displacement measurement was accomplished using a Schaevitz displacement transducer that was activated by a Schaevitz Carrier Amplifier Indicator model Tr-100. The amplifier was calibrated using a dead weight calibrated spring balance. Although the calibration remained fairly constant the apparatus was calibrated before and after each set of tests to ensure strict results and observe whether foreign matter had interfered with the free movement of the plate. A typical calibration chart is shown in Figure 3.3.

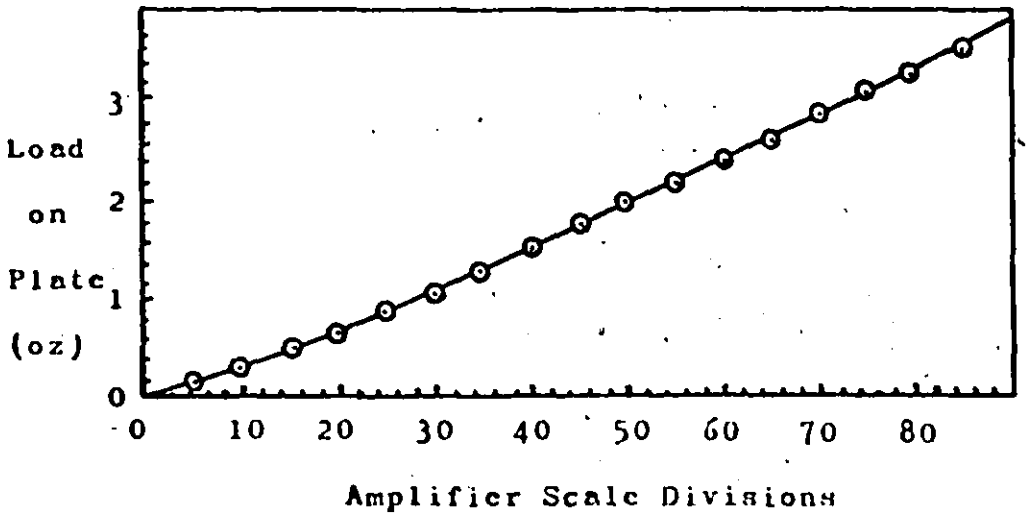

Figure 3.3 Typical Force Calibration of Displacement Tranducer Amplifier

Calibrating the transducer readout to provide direct drag force measurement eliminated the necessity of converting displacement measurements. The transducer was found to be insensitive to temperature changes. The ambient temperature fluctuated between 60 and 70

degrees F during the 4 month experimentation period but the calibration charts did not alter.

The free stream velocity and velocity profile measurements were made using Novar-Nixon Streamflow velocity meters. Use is made of the fact that electrical conduction in a fluid is a function of the speed of rotation of a propeller device which displaces the fluid with its vanes. The velocity probe determines the average flow velocity over a 1/2 inch diameter circular region every second, ten seconds, or continuously depending on the function selection in the display amplifier unit. The probe is attached to a three dimensional vernier traverse mechanism located on the flume top rails as shown in Figure 3.2. Appendix I deals with the calibration of these probes and discusses their merits.

The injection apparatus consisted of a 4 inch diameter, 4 litre capacity plexiglass tube. It was calibrated in 100 ml graduations and was connected to a finely regulated pressure supply. The injection rate was controlled by adjusting the variable pressure supply and measured by noting the elapsed time, for a known volume of injection fluid to pass, using a stopwatch, The injection system was capable of ejecting up to 60 ml/sec of highly viscous 2000 wppm polymer concentrations with correspondingly higher rates possible for less viscous fluids. The greatest injection rates used were 50 ml/sec for most of the tests.

CHAPTER IV

EXPERIMENTAL PROCEDURES:

4.1 General Method

The flume flow conditions were adjusted such that the required free stream velocities were obtained along with an adequate depth such that the velocity profiles were not affected by a shallow ceiling. A 12 inch minimum depth was insured for all the tests although greater velocities might have been attained with a lower depth. Accelerated flow and skewed velocity profiles were encountered with the shallow depth tests and drag results could not be compared to theoretical predictions, whereas the 12 inch minimum depth requirement ensured adherence to theoretical drag relationships.

Once the flow condition was well established the drag on the plate was noted from the displacement transducer display. Injections of 125, 250, 500, 1000, and 2000 wppm were made at numerous injection rates ranging from 0 to 60 ml/sec. Injection solutions were prepared by diluting 2000 wppm concentrations of Reten 423 (Union Carbide), Seperan AP-30 (Dow Chemical), Polyhall 295 (Stein-Hall), Polyox WSR-30 and an equimolar micellar solution of CTAB and 1-napthol. Five sets of data were obtained by noting the drag modifications due to injecting each of the above solutions into the free stream adjacent to the flat plate test section. The free stream velocities

were varied between 1.5 and 5.6 fps.

4.2 Ablative Coating

The coatings, which were produced by adhering a polymer coating to 6 by 24 inch strips of blotting paper, were prepared three different ways. The first involved soaking the blotting strips in 20,000 wppm solutions of Reten 423, Reten 423 was applied directly to the blotters as an alcohol suspension whereupon their entire surfaces were wetted in the second method and in the third the poymeric powder was sprinkled directly unto the wet blotters.

The effects of uncoated blotters on the test section were checked prior to using the coatings. The uncoated blotters were substituted in place of the ablative coatings and the resultant drag characteristics were noted as may be seen in the initial sections, prior to t=o, of Figures 5.7 and 5.8. In all cases the blotters were allowed to dry before installation and were fixed to the plate using rubber cement.

An investigation into the effective concentration of the polymer solution in the vicinity adjacent to the blotters was attempted by collecting samples over their surfaces and comparing the sample viscosities to known ones. The results were interesting but not very substantiable as large volume samples could not be taken for drag effectiveness studies and there is evidence which indicates polymer may lose effectiveness with

degradation but not necessarily viscosity.

The blotters were also allowed to dry after a test and then reused. The tests were conducted with free stream velocities of 4 fps for periods of time up to 1 hour in duration to investigate the blotter degradation characteristics.

4.3 Polymer Solution Preparation

The polymers used were named in section 3.1. All were prepared similarily, by dispersing a weighed quantity of polymer in alcohol and then gently stirring it into a large container of water such that a 2000 wppm concentration was obtained.

Although the solutions were used within 18 hours of preparation no noticeable differences were present with Reten 423 over a three week period of storage.

4.4 Micelle Solution Preparation

The solutions were prepared by first dissolving the weighed quantity of CTAB in water, to produce a 5080 wppm total concentration with a solution of 1-naphthol which had been previously dissolved in alcohol and added drop by drop as the whole mixture was being stirred. An insoluble precipitate could be obtained if the 1-naphthol-alcohol solution was added too quickly. Sunlight seemed to give the solutions a bromide colouring. Aging characteristics of the solutions were unknown, although quantities left in storage were found to lose all drag

reducing properties, hence the solutions were used immediately after their preparation.

4.5 Velocity Profiles

The velocity meter described in Section 3.3 provided a direct measurement of velocity profile over the plate. When required, profiles were taken by placing the probe head as near the plate surface as possible and raising it progressively with the vernier, noting velocities. As the head was 1/2 inch in diameter average velocities could not be obtained closer than .25 inches from the test plate surface. Although the viscous sublayer could not be investigated good profiles were obtained both during injection of additives and at normal free stream conditions. The viscous sublayer thickness was determined theoretically for flows with no injection and taken to be twice that for flows with injection as suggested by Hoyt(1). The fluid velocities at these distances from the wall were obtained theoretically and plotted on the velocity profile plots. A linear velocity relationship was assumed within the viscous sublayer.

CHAPTER V

EXPERIMENTAL RESULTS:

All the drag measurements were obtained from the flat plate which had a surface area of 2 square feet. The data, to be presented, uses as the indication of drag, drag on the plate in oz/ft^2 which was obtained by halving all the data obtained from the 2 ft^2 plate.

Figure 5.1 presents the drag characteristics of the apparatus and compares them to theoretical values as predicted by equation 5.1 which considers laminar flow over the initial length of a flat plate up to a critical Reynolds number. The critical Reynolds number used was 300,000, being the lowest possible for this situation as described by Schlichting(16).

$$F_{tot} = \left(\frac{1.328}{Re_L}(Re_x)_{cr}^{\frac{1}{2}} + \frac{0.074}{Re_L^{\frac{1}{5}}} - \frac{0.074}{Re_L}(Re_x)_{cr}^{4/5}\right)\left(\tfrac{1}{2}\rho U_\infty^2 L\right) \qquad (5.1)$$

Also shown in Figure 5.1 are the Drag relationships for turbulent flow with no laminar portion assumed as defined by Equation 5.2,

$$F_{tot} = 0.036\ \rho\ U_\infty^2\ L\ /\ Re_L^{1/5} \qquad (5.2)$$

and complete laminar flow as shown by,

$$F_{tot} = 0.644\ (\mu\ \rho\ U_\infty^3\ L)^{\frac{1}{2}}. \qquad (5.3)$$

The drag is calculated by evaluating each of the above equations for an 8 foot long plate and then for a 4 foot long plate. The difference results in the drag on the last 4 feet of an 8 foot plate. The above

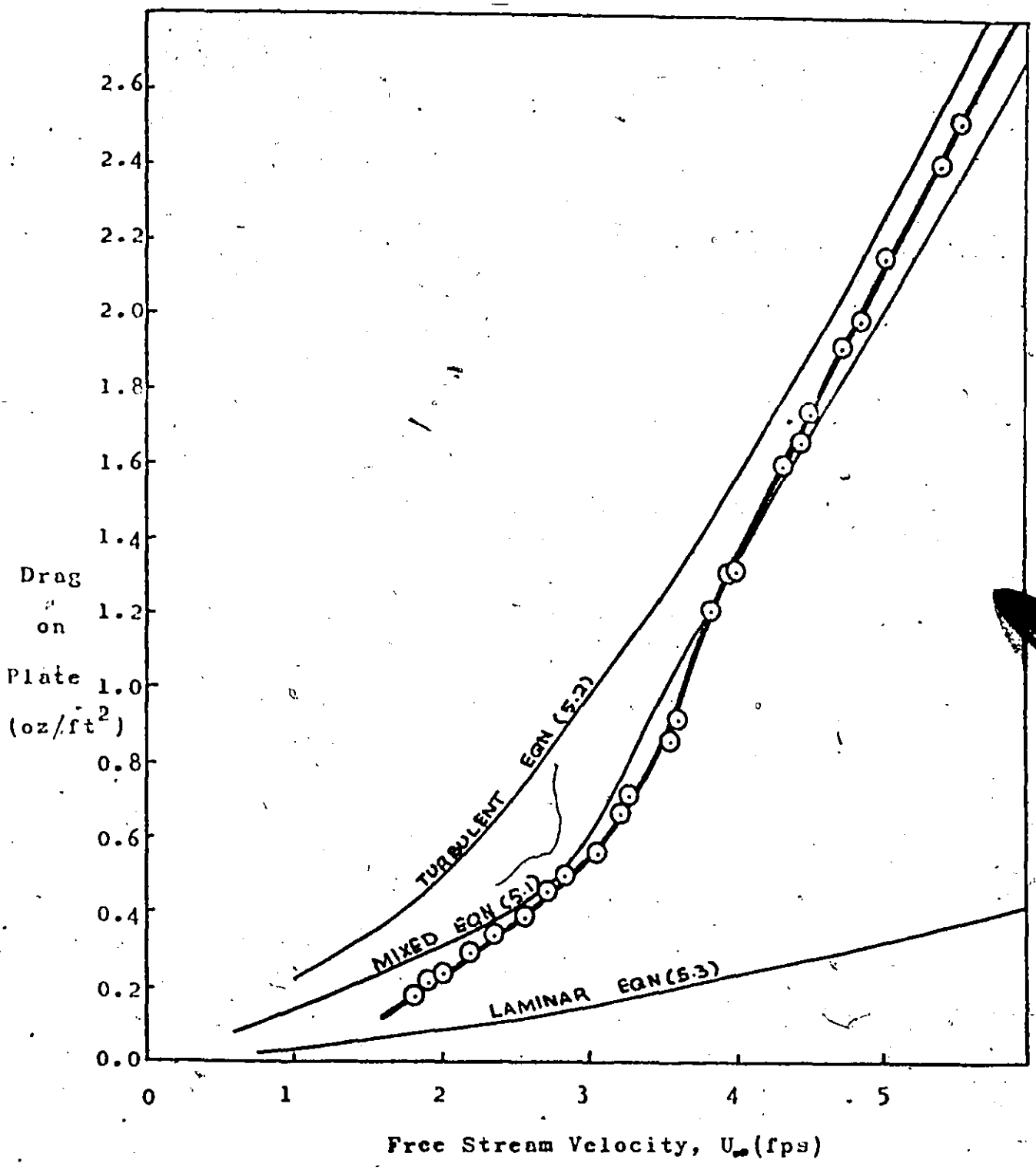

Figure 5.1 Comparison of Experimental Drag Measurements with Theoretical Relationships

equations are for a plate of unit width. Since the experimental plate is 1/2 foot wide, the results thus

obtained must be halved.

The apparent agreement between equation 5.1 and the experimental data indicates that transition occurs at a Reynolds number near 300,000 and that a turbulent boundary layer is ensured over the test section even at free stream velocities of 2 fps, as well as indicating that the apparatus is measuring drag reasonably well.

The 5.2 series of figures present the drag reduction data obtained using Reten 423 as a function of injection rate and concentration, and free stream velocity. The ΔD, or change in drag figures, were obtained by subtracting the injection drag values from the non-injection drag values and dividing them in half to get the drag per square foot. The reproducibility of the data in Figure 5.1 was virtually 100 per cent and absolute drag values may be obtained by subtracting the 5.2 ΔD values from the

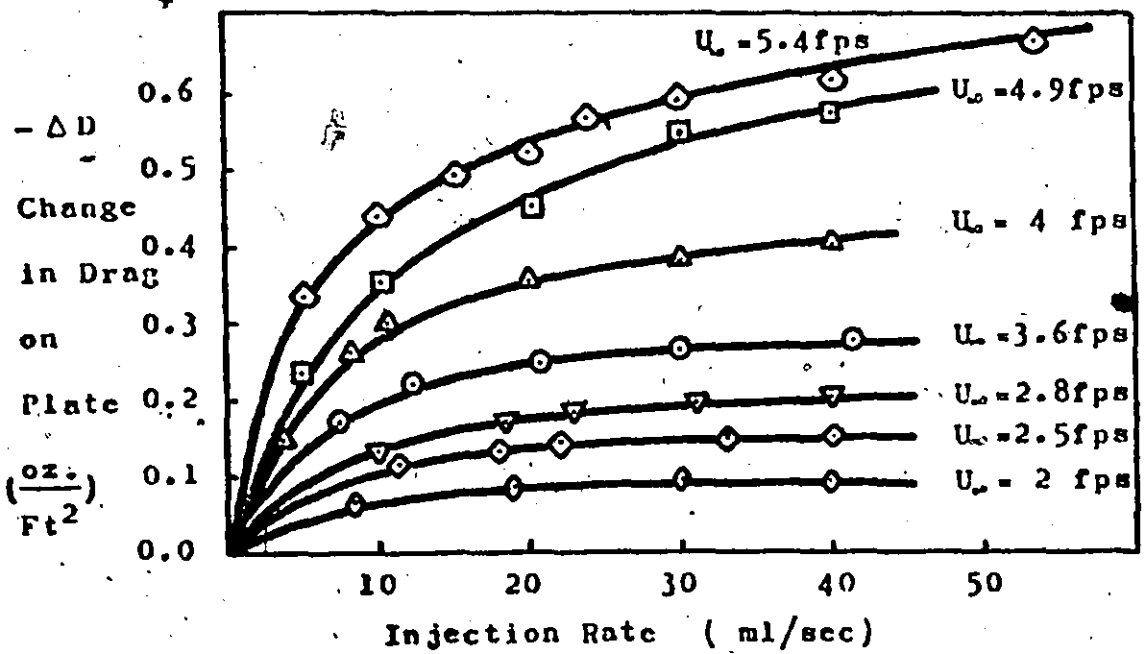

Figure 5.2a Drag Reduction Data for 2000 wppm Reten 423

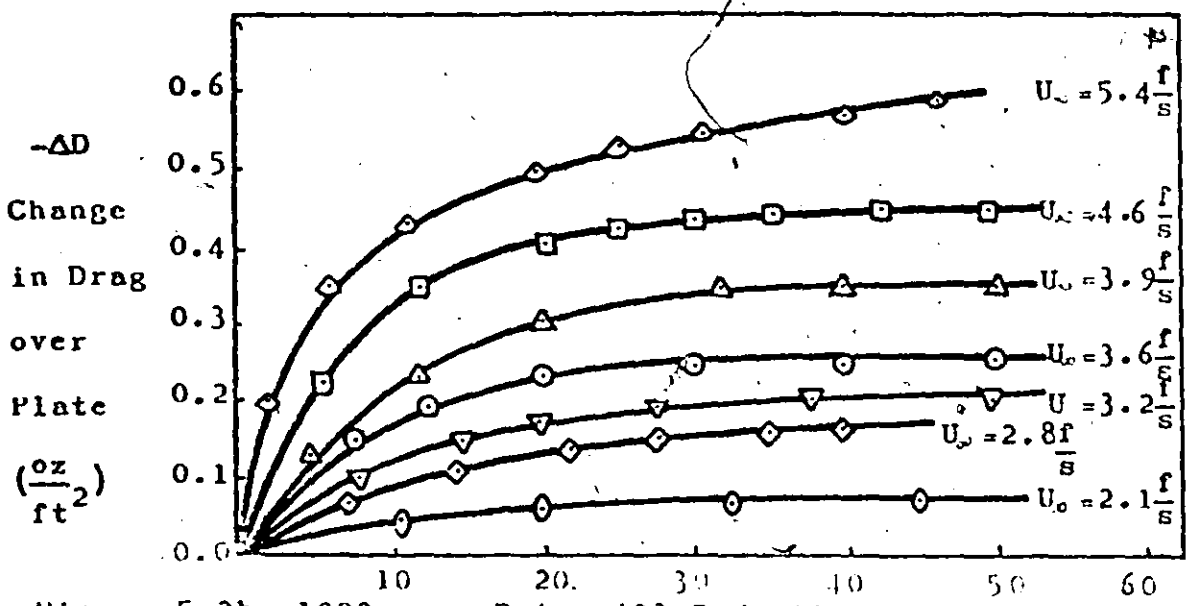

Figure 5.2b 1000 wppm Reten 423 Injection Rate (ml/sec)

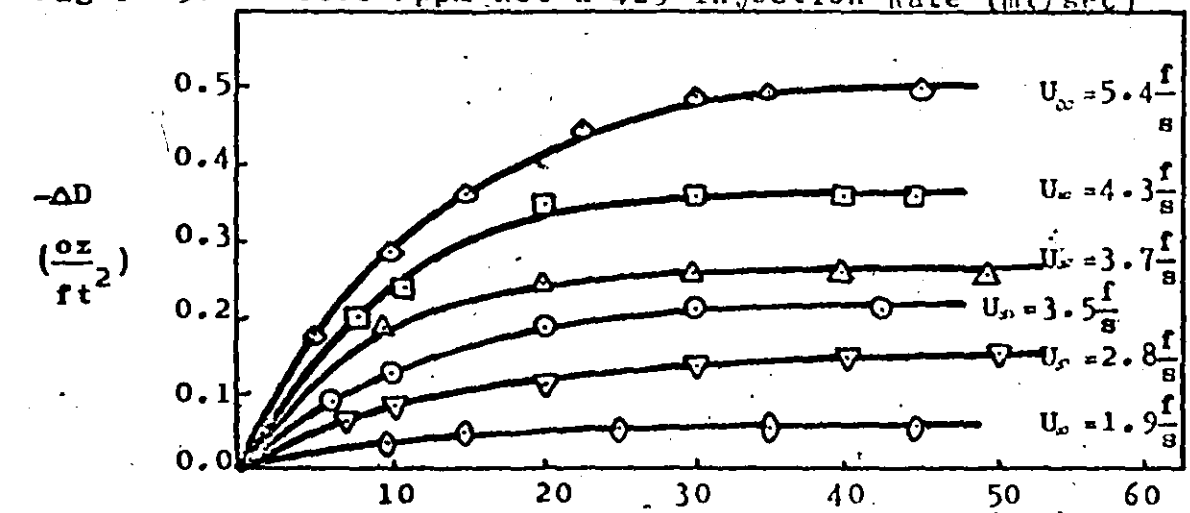

Figure 5.2c 500 wppm Reten 423 Injection Rate (ml/sec)

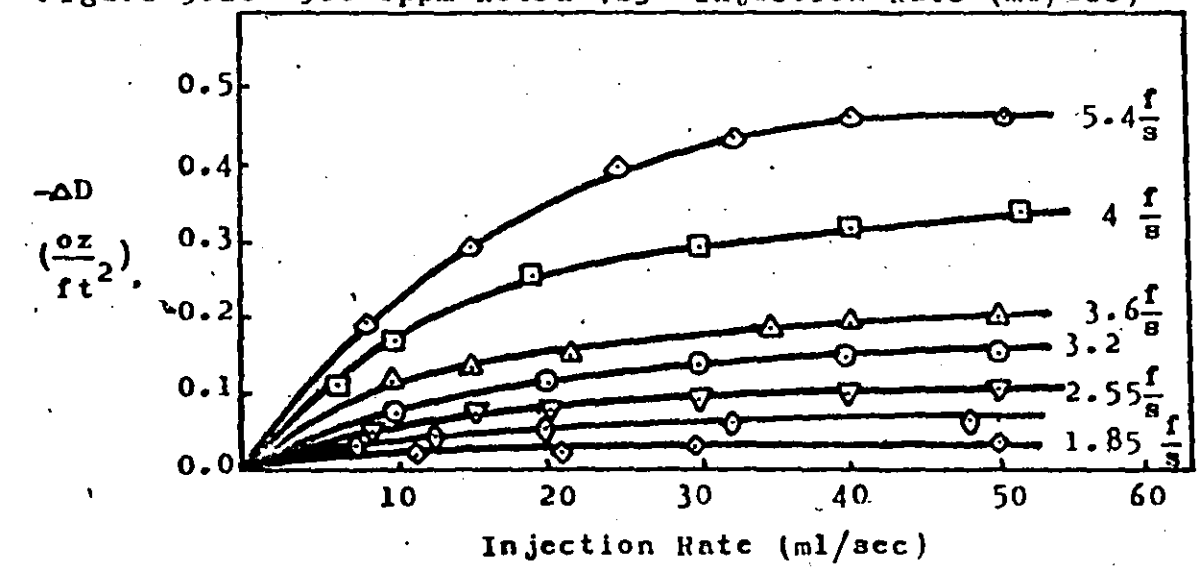

Figure 5.2d Drag Reduction Data for 250 wppm Reten 423

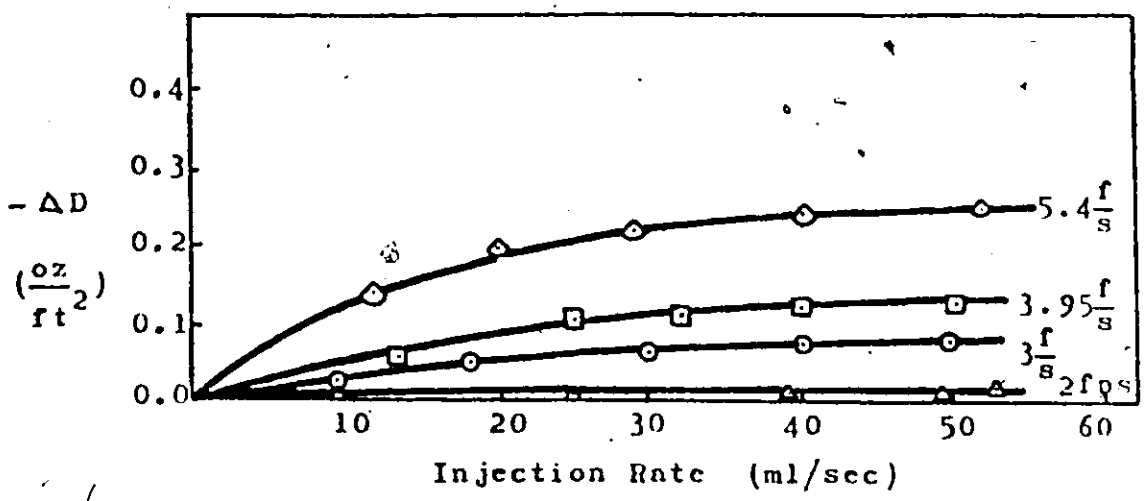

Figure 5.2c Drag Reduction Data for 125 wppm Reten 423

corresponding values there.

The diagrams in Fig. 5.2 show the effect of increasing velocity for a given injection rate and concentration. The 5.3 series of figures present the drag reduction data obtained for Seperan AP-30 and Polyhall-295. These figures are plotted for constant velocities and show the effect of increasing concentration at specific injection rates.

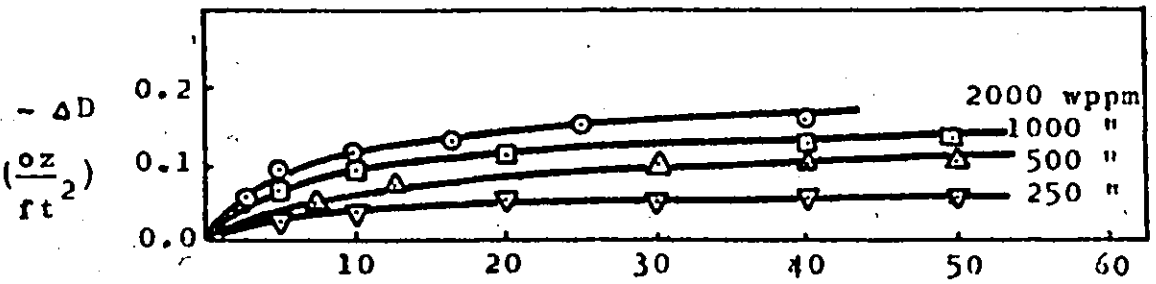

Figure 5.3a Polyhall-295 at U_∞=2.8 fps, Injection rate(m/s)

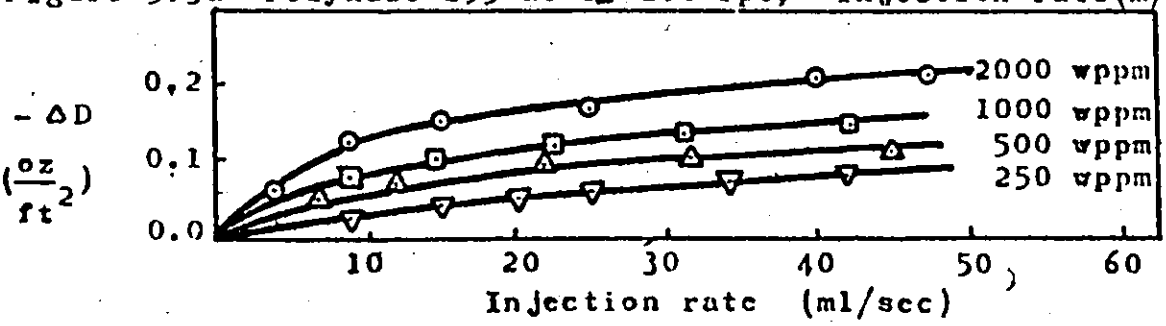

Figure 5.3b Drag Reduction Data for Seperan AP-30 at a Free Stream Velocity of 2.8 fps.

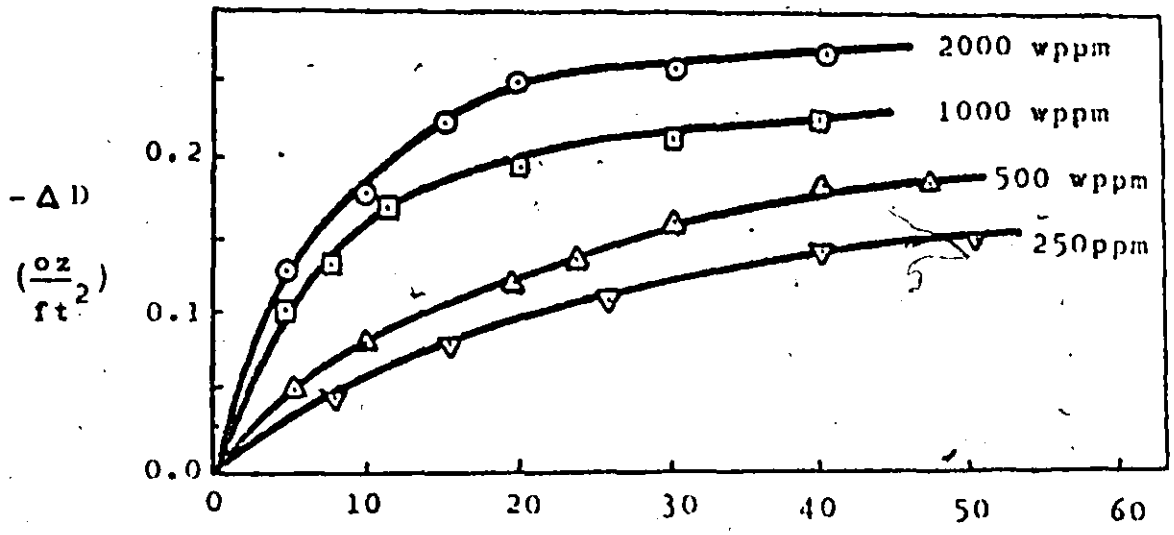

Figure 5.3c Polyhal-295 at U_∞ = 3.8 fps Injection Rate (ml/s)

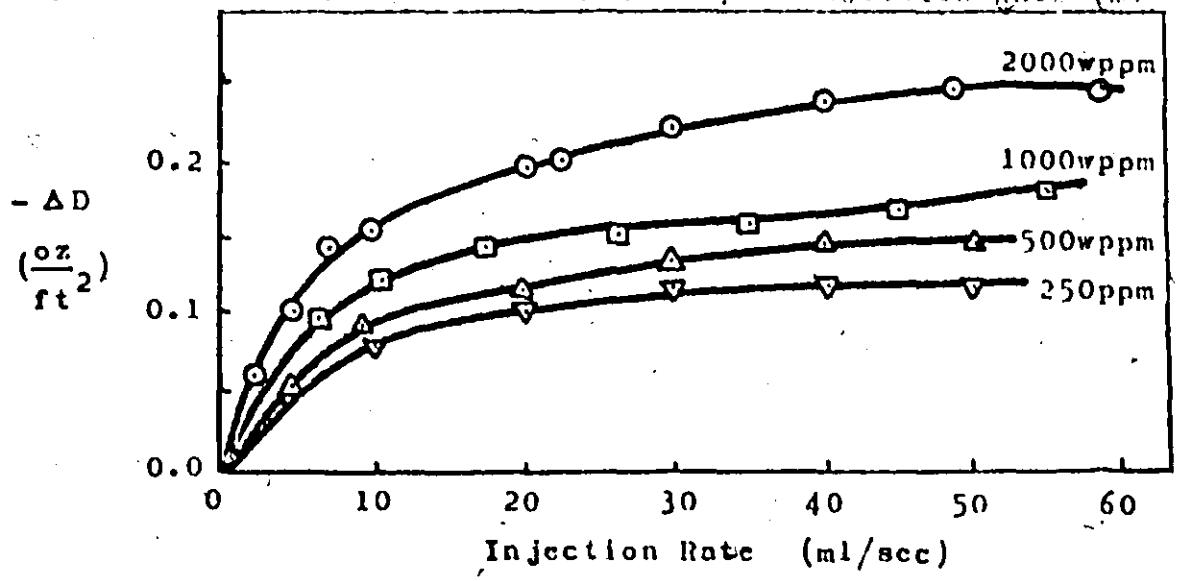

Figure 5.3d Drag Reduction Data for Seperan AP-30 at a Free Stream Velocity of 3.8 fps.

Absolute drag values may be obtained from the 5.3 figures by using Figure 5.1.

Of the polymers tested Polyox-WRS 30 was found to be least effective at the concentrations tested. Drag reduction effectiveness was found to increase with concentration but a 2000 wppm concentration was the maximum tested and it is apparent that although greater concentrations would produce more drag reduction they would also

decrease economical employment. Figure 5.4 shows the effect of 2000 wppm Polyox WSR 30. Although data was available for lesser concentrations it is not presented as the modifying effects were very slight.

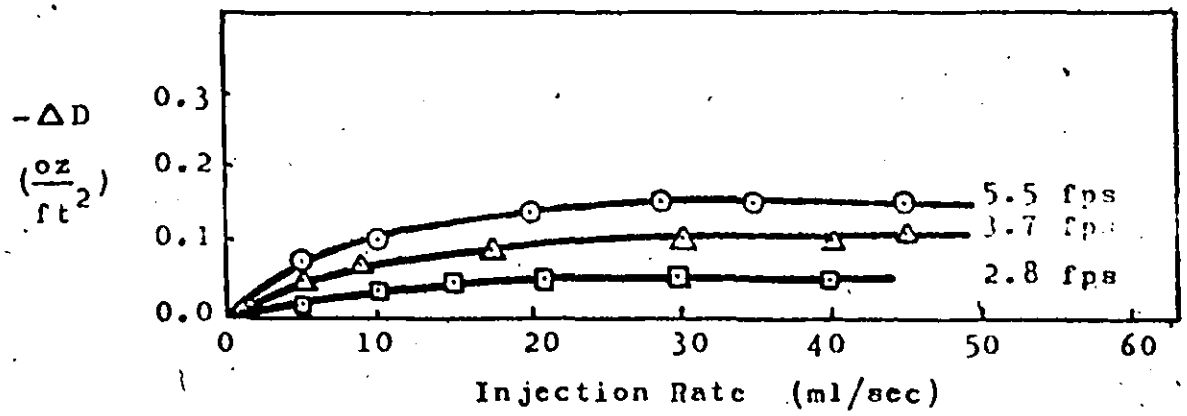

Figure 5.4 Drag Reduction Data for Polyox WSR 30

It should be noted that Reten, Seperan, and Polyhall are all polyacrylamides and that Polyox is a polyethylene-oxide. Polyethylene oxide is a completely linear molecule whereas the polyacrylamides are branched. Although Polyox WSR 30 has been found less effective than the polyacrylamides other polyethylene oxides may be more effective. Hoyt(1) compared the concentrations of material required to achieve 67 percent drag reduction in pipe flow at Re=14000 and stated that 10 wppm of Polyox WSR 301, (which was not used for these experiments), would be equivalent to Polyhall 295 at a concentration of 20 wppm.

A micellar type of material, Cetyltrimethylammonium bromide-1-naphthol (CTAB), was also examined for drag reducing characteristics, the results of which are shown in Figure 5.5.

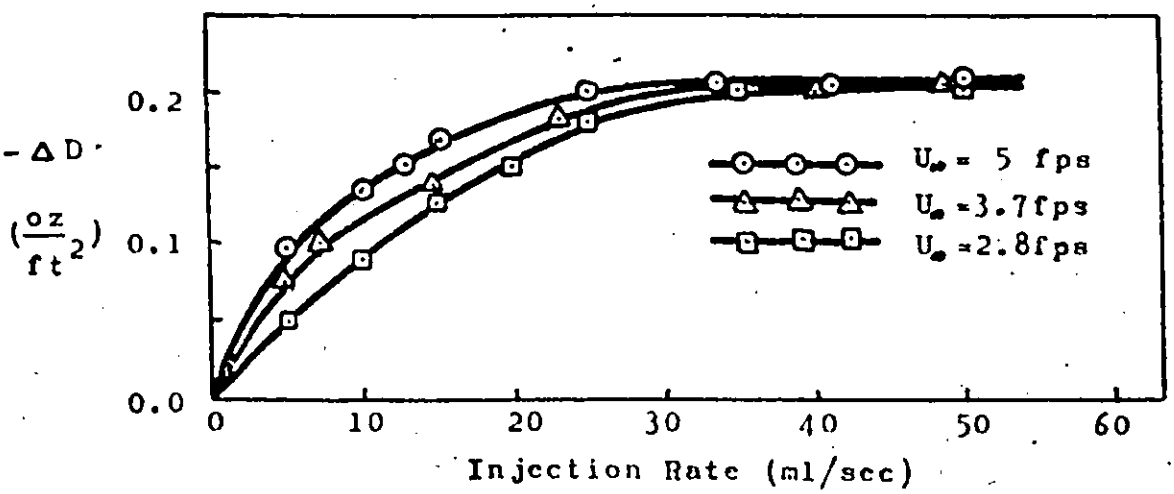

Figure 5.5 Drag Reduction Data for an equimolar solution of Cetyltrimethylammonium bromide and 1-naphthol to give a total concentration of 5080 wppm.

During the course of experimentation the recirculating water supply for the flume was foulled with fine aluminum powder by another researcher. The particles were a few ten thousandths of an inch in diameter and their concentration was estimated to be approximately 200 particles per cubic inch of water. Figure 5.6 shows how the aluminum additive modifies the drag as obtained in Figure 5.1.

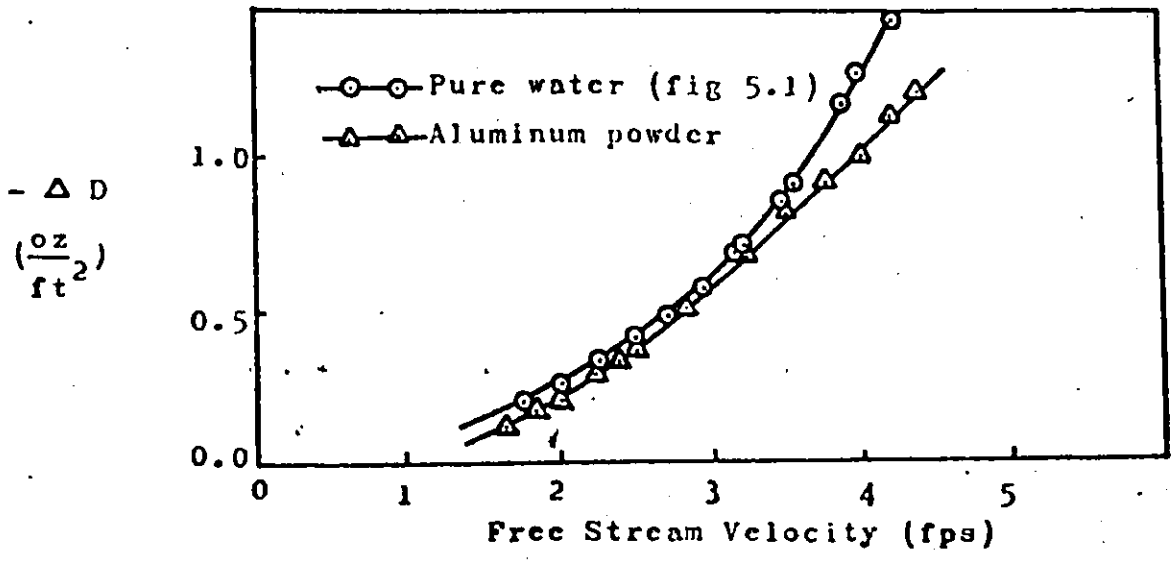

Figure 5.6 Effect of a Homogeneous Aluminum Powder Solution on the drag over a Flat Plate

Further experimentation was, of course, resumed after removing the aluminum powder from the system.

The temperature of the injection fluid was also found to have an effect on the measured drag in that differential expansion (or contraction) occurred. The portion of the plate which provided the frame to suspend the test section did not have contact with the injections thus it remained at the free stream temperature. The test section rapidly assumed the injection fluid temperature during injection and its length was modified. As the measuring instrumentation was housed by the frame portion of the plate a displacement could have been noticed by just altering the temperature of the test section. It was found that keeping the injection fluid at the free stream temperature avoided this effect and all the solutions were brought to the free stream temperature before use.

Tests also indicated that the drag characteristics remained unaltered by injecting water into the boundary layer over the test section. Since water was the solvent for all the additives tested it must be assumed that whatever modifications took place were due to the presence of the additives themselves.

Figure 5.7 shows the drag modification characteristics of an ablative surface mounted directly upstream of the test section. The initial section of the drag reduction curve, up to t=0, was obtained using an untreated blotter to see how its presence affected the drag resulting

over the test section of the flat plate. The experiment was conducted at U_∞ = 4 fps, and it may be noted that a slight increase in drag is experienced over that plotted in Figure 5.1. The dummy blotter was then removed and the coated blotter set in its place. At t=0, the flow was started and brought up to the free stream velocity of 4 fps as quickly as possible. The resultant drag modification is interesting in that it continues for a long time. As the ablative coating was wetted, it grew a geletinous covering which adhered to the surface and would not wash off unless scraped. The experiment was discontinued after 1 hour and the coating was allowed to dry. The geletinous coating dried up and the test was repeated. The same effect was noticed as in the first test. No time trials were performed but the blotters seem to have a very long life expectancy.

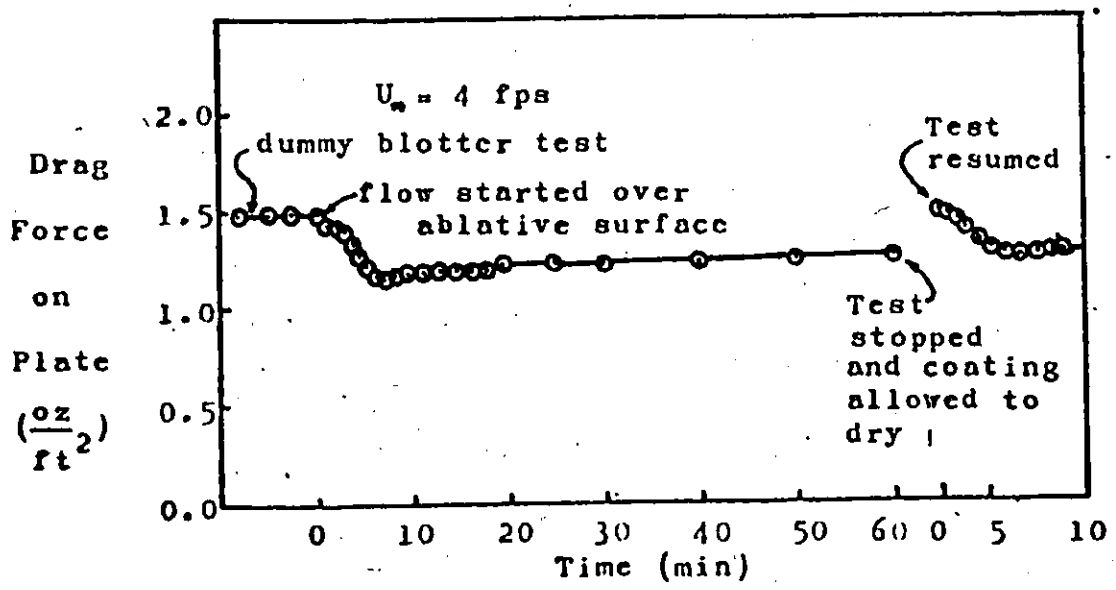

Figure 5.7 Drag Reducing Effects of Ablative Surface Mounted Directly Upstream of Test Section

Figure 5.8 shows the results of the same experiment as described for Figure 5.7 except that the ablative surface, which measured $\frac{1}{2}$ by 2 feet was mounted on the upstream half of the test section.

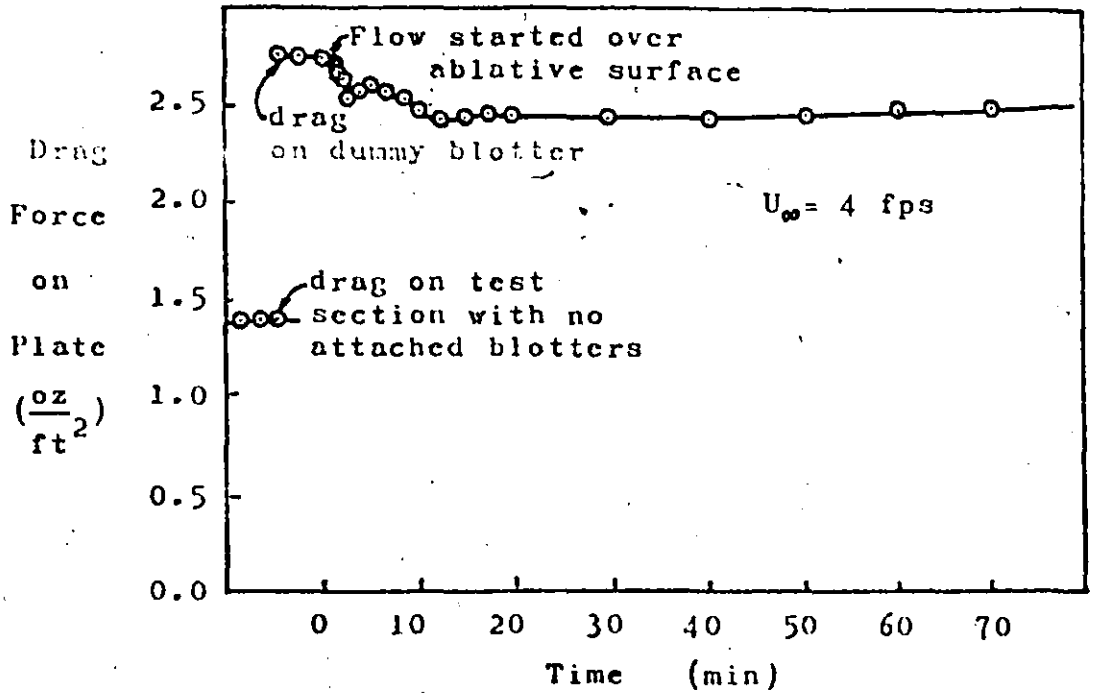

Figure 5.8 Drag Reducing Effects of Ablative Surface Mounted Directly On Test Section.

During the test illustrated by Figure 5.8 a number of fluid samples were obtained at various points over the test section using a pitot tube. The viscosities of the samples were obtained using a Brookfield cup and cone viscometer and compared to those of known concentrations of Reten 423. It is not known whether degradation, if any, occured and it is difficult to substantiate equating viscosities to concentrations without performing actual

drag measuring experiments which would require much larger amounts of sample. The results of that investigation along with rheological data for Reten 423 are presented in Appendix VI.

CHAPTER VI

DISCUSSION OF RESULTS:

This research was concerned with producing usable drag reduction data. This laboratory is also investigating the diffusivity of polymer injections in liquid boundary layers. The results of that particular investigation may extend the data presented in Chapter V to allow predicting drag reductions over greater lengths than 4 feet downstream of the injection slit. As the experiment was conducted with a four foot long plate, it must be understood that when drag forces are given per square foot they were obtained by dividing the total drag force on the plate by two. The exact distribution of drag over the length of the plate is not known although an attempt to determine it was made by doing velocity traverses during injections and estimating the drag from a momentum thickness analysis as shown in Appendix II.

Although data is scarce, it is known that polymer concentration decreases with distance downstream of injection and that the amount of drag reduction is concentration dependent. Dye injection studies indicated however, that the injection remains fairly coherent once a basic amount of diffusion, which is free stream velocity dependent, had occurred. The coherent injection travelled the length of the flume upon leaving the test section (about 10 feet) but it is not well established whether the dye, diffusing into the free stream, gave a false impression to the limit

of the injection boundary by diffusing beyond perception. A photographic analysis is given in Appendix IV.

Of prime interest in this study was how the polymer concentration and its injection rate affected the drag modifications. The data presented in the 5.2 series of figures may be condensed into Figure 6.1. This condensation is possible because the data presented in Figure 5.2 indicate that injecting a 2000 wppm concentration of polymer at 20 ml/sec is equivalent to injecting 500 wppm at 40 ml/sec or 2000 wppm at 10 ml/sec with respect to the total drag reduction possible. This is especially true with the more water soluable polyacrylamides.

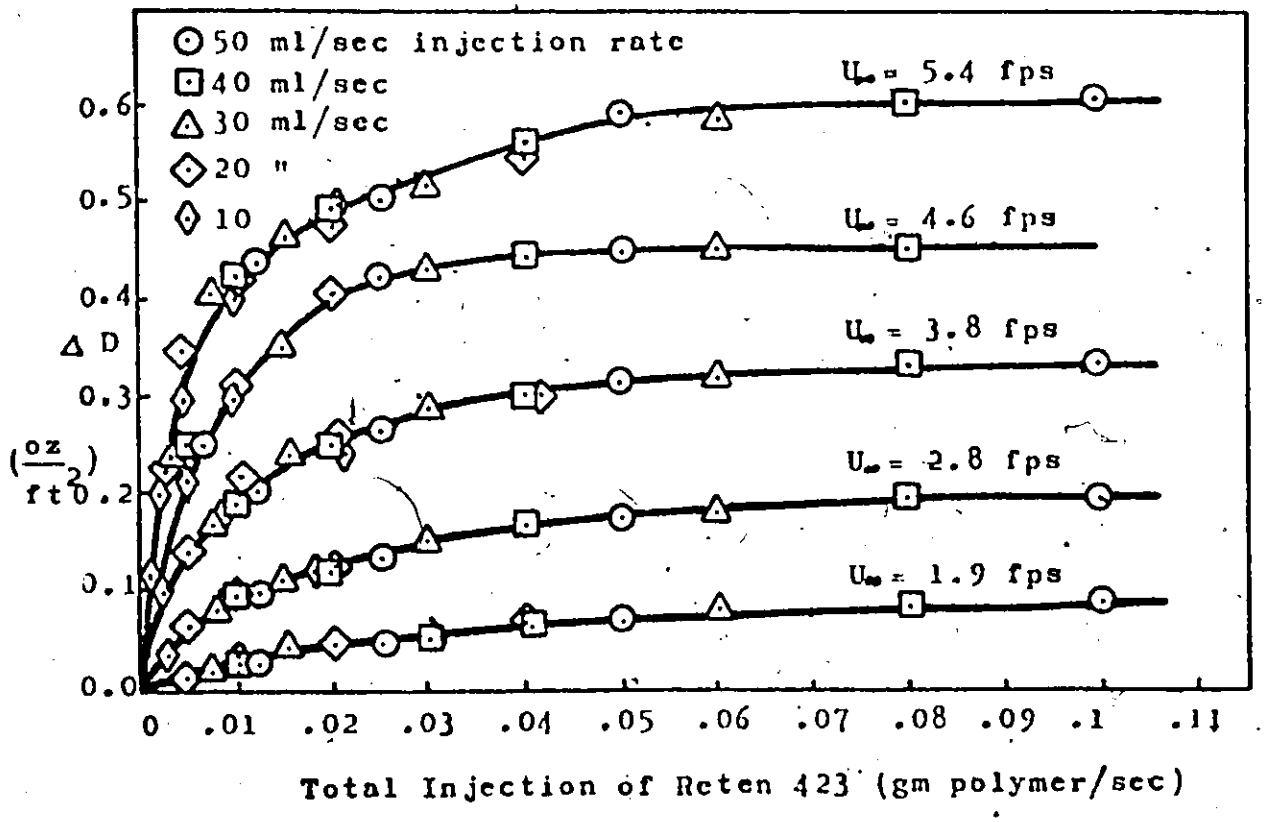

Figure 6.1 Drag Reduction Characteristics of Reten 423

The total injection, as shown in figure 6.1 is obtained by taking the product of the injection rate and the additive concentration shown in each diagram of Figure 5.2. This operation yields units of wppm-ml/sec, but since the molecular weight of polymer solutions is essentially the same as that for water, the units become wppm-gm/sec. Injecting 2000 wppm at 50 ml/sec introduces 100,000 wppm ml/sec gm/ml or 0.1 gm/sec of polymer into the boundary layer over the plate.

Increasing the injection concentration to the point where additional viscous drag forces will outweigh the additional drag reduction provided by adding polymer, should be a function of the total concentration present. The data, published by Tulin and Wu(14), indicates that maximum drag reductions occur at injection rates of approximately 55ml/sec/½ft plate width. This optimal injection rate does not vary enough to compensate injection concentration variance in a direct ratio. Their data indicates a ratio of 3 between the optimum injection rate of 50 wppm and 800 wppm, whereas, 16 times more 50 wppm concentration solution should be injected to introduce the same amount of polymer as would an 800 wppm solution. Internal flow data, some of which is shown in Appendix V, indicate that optimum reduction is in fact concentration dependent. Thus the apparent optimal concentration variance over a flat plate may be due to concentration gradients existing along its length.

Very few of the injection rates presented in Chapter V exceed 50 ml/sec and although most of the corresponding drag reduction rates have levelled, none have started to decrease. In fact the drag reduction curves of 2000 wppm Reten 423 are still increasing at injection rates greater than 50 ml/sec when subjected to free stream velocities greater than 4 fps. The drag reduction characteristics observed by Tulin and Wu([1]), for 800 wppm concentrations, were found to decrease above injection rates of 20 ml/sec. It must be noted however, that they were using Polyox WSR-301, 10 wppm of which is, reported by Hoyt([1]), as effective as 20 wppm of Polyhall 295. If Figure 5.2b is compared to Figure 5.3c it may be noted that 2000 wppm Polyhall 295 give reductions equivalent to 1000 wppm Reten. As the actual drag modification occurs over the plate, the amount of Reten 423 present in the boundary layer should be compared to the amount of Polyhall required to produce the same effects there. Figure 1?.2 shows a 9.5 wppm concentration of Reten in the boundary layer for a free stream velocity of 3.8 fps and an injection rate of 50 ml/sec using a 1000 wppm initial concentration. Under these same conditions a 2000 wppm concentration of Polyhall was found to have the same drag reducing effects. Thus a 20 wppm concentration of Polyhall is equivalent to a 10 wppm concentration of Reten. Hence Reten 423 and

Polyox WSR-301 may have the same effectiveness in equal concentrations.

It must also be noted that the Tulin and Wu(14) experiments were conducted at a free stream velocity of 8 fps. The 5.2, 5.3, and 5.4 Figures all indicate that the drag reduction curves begin to level off at progressively increasing injection rates with increasing free stream velocities. This effect indicates that the polyacrylamides tested may offer less viscous drag than Polyox WSR-301 since even at lower free stream velocities much greater concentrations injected into the boundary layer did not cause the drag reduction curves to decrease.

The viscosity of Retan 423 does increase with concentration, as shown in Figure 15.3, so a decrease in drag reduction is expected in all the 5.2 Figures at particular injection rates. These injection rate limits may be surpassed in trying to obtain any of the Total Injections referred to in Figure 6.1. This could produce points which fall below the indicated data. Hence injection rates greater than 50 ml/sec should not be used in predicting the Total Injections.

It also seems that the ultimate reductions have been fairly well reached in Figure 6.1 and greater Total Injections may result in lower drag reductions, thus Total Injection Rates should remain below .11 gm polymer per second.

The few points which deviate substantially from the curves in Figure 6.1, do so because they originated from high concentration, low rate injections, at relatively high free stream velocities; all being conditions which prevent good mixing with the boundary layer liquid and result in less drag reduction.

The first attempt at producing an equation for Figure 6.1 resulted in a linear approximation which is shown in Equation 6.1 and fitted to Figure 6.1 in Figure 6.1b.

$$\left.\begin{aligned} \Delta D &= (0.017 + 0.05\, Q_{in})\, U_\infty^2 \quad \text{for } Q_{in} \geq 0.02 \\ \Delta D &= (0.01 + 0.4\, Q_{in})\, U_\infty^2 \quad \text{for } 0.5 \leq Q_{in} \leq 0.02 \end{aligned}\right\} \quad (6.1)$$

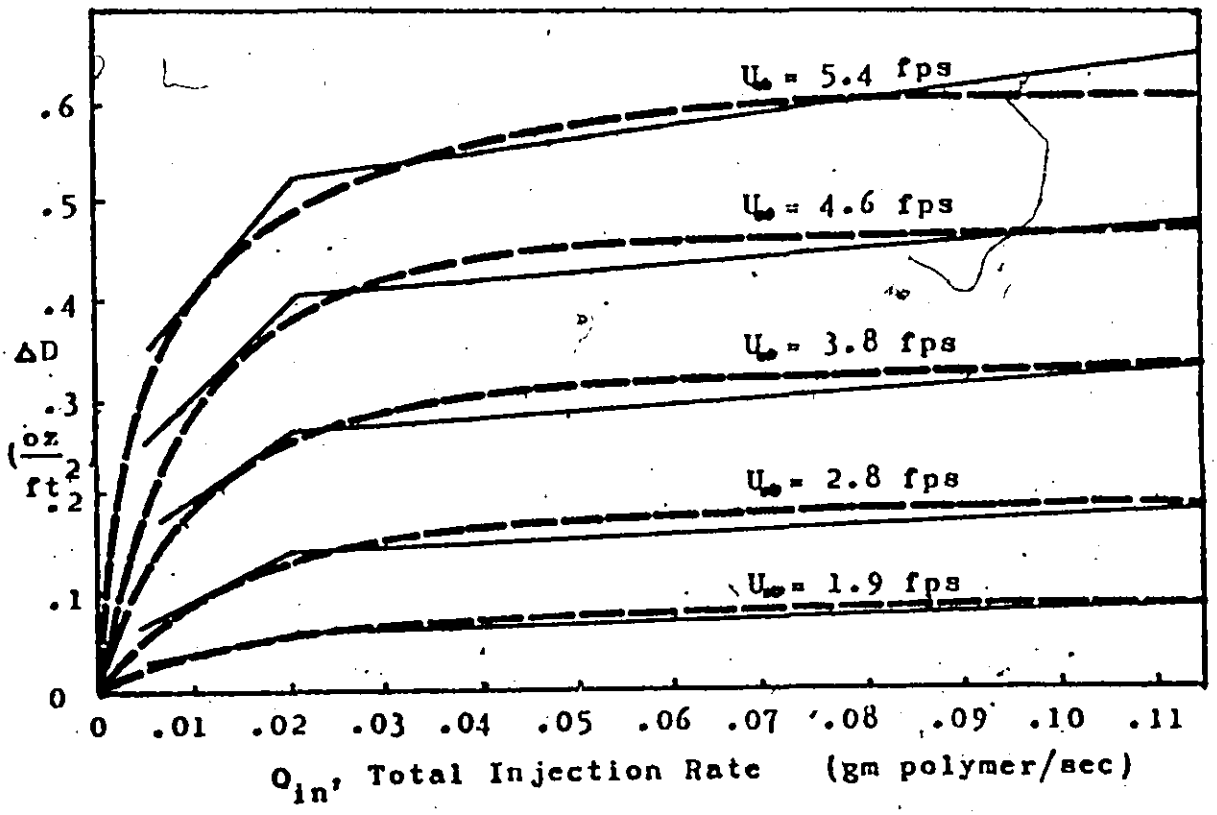

Figure 6.1b Correlation between Figure 6.1 and Linear Approximation Equation 6.1

The linear approximation of Figure 6.1b suggests a 2nd or 3rd order polynomial may fit the experimental data quite well but it is interesting to note that the drag reduction is a rather simple function of the total polymer injection rate and, as expected, the free stream velocity. Similar procedures seem applicable for the other polymers which were tested and perhaps a series of similar equations may be generated employing a constant which would vary from polymer to polymer depending on its effectiveness.

Figure 6.2 is obtained from the concentration analyses presented in Appendices III and IV for Retan 423. Grouping towards the 17 wppm asymptote agrees with the internal flow data conclusion that maximum drag reduction is obtained at a 20 wppm concentration, as shown in

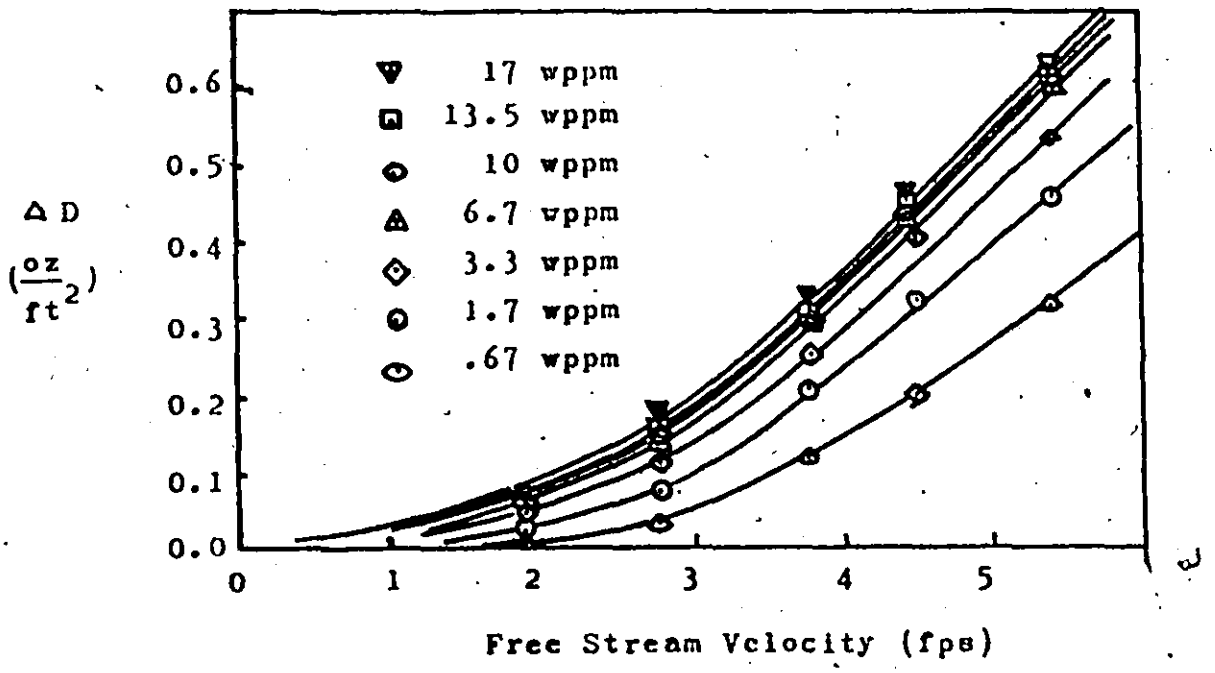

Figure 6.2 Approximated Boundary Layer Polymer Concentration Effects on Drag Reduction

Appendix V. Ejections which would have produced concentrations greater than 20 wppm were not attained at the higher free stream velocities but where exceeded at low free stream velocities there is no indication of less drag reductions although there is no apparant increase either. It is expected, however, that the curves shown in Figure 6.1 and 12.2 will begin to drop once concentrations of about 30 wppm are exceeded.

Maximum effects are probably attained with a 20 wppm concentration but since the drag is being measured over a 4 foot length of plate a consistant concentration cannot be assumed over it. The constant concentration analysis presented in Appendix III does not account for a distribution providing 40 wppm concentration at the leading edge of the test section and 0 wppm at the trailing edge. This would not produce an average 20 wppm concentration over the whole plate but would have the leading edge being acted upon by a concentration which produces less drag reduction than that at the trailing edge. As long as the relative proportions of these two factors remain balanced the total drag reduction over the plate will remain unchanged. It is expected however that once more than half of the plate is experiencing a flow with concentration greater than 20 wppm a decrease in drag reduction will occur and Figure 6.2 will have curves of greater concentration than the asymptotic value producing less drag reduction.

At 5.4 fps, Figure 6.2, indicates that a 10 times dilution of a 17 wppm concentration results in only a 30% loss in drag reduction. This effect becomes more pronounced with increasing free stream velocity. It is realized that more drag reduction is possible at higher U_∞ but it seems that the possible drag reduction decreases due to dilution will also be lesser.

Since trace particles produce such significant amounts of drag reduction it seems that injections over very large lengths should be very effective. Injecting concentrations much larger than necessary at the leading edges of large surfaces would produce some drag reduction, then as dilution progressed, there would be an increase in drag reduction until the optimum concentration was reached whereupon there would be a decrease until no trace remained. From submerged jet studies, White(9), and from the dye studies in Appendix IV, it seems that even though there is a fairly rapid dilution occuring near the injection point, this dilution reaches a concentration at some point downstream which does not dilute very rapidly with distance. It is suggested that a study be undertaken to determine the concentration of injected solutions 30 or more feet downstream of injection, especially at higher free stream velocities.

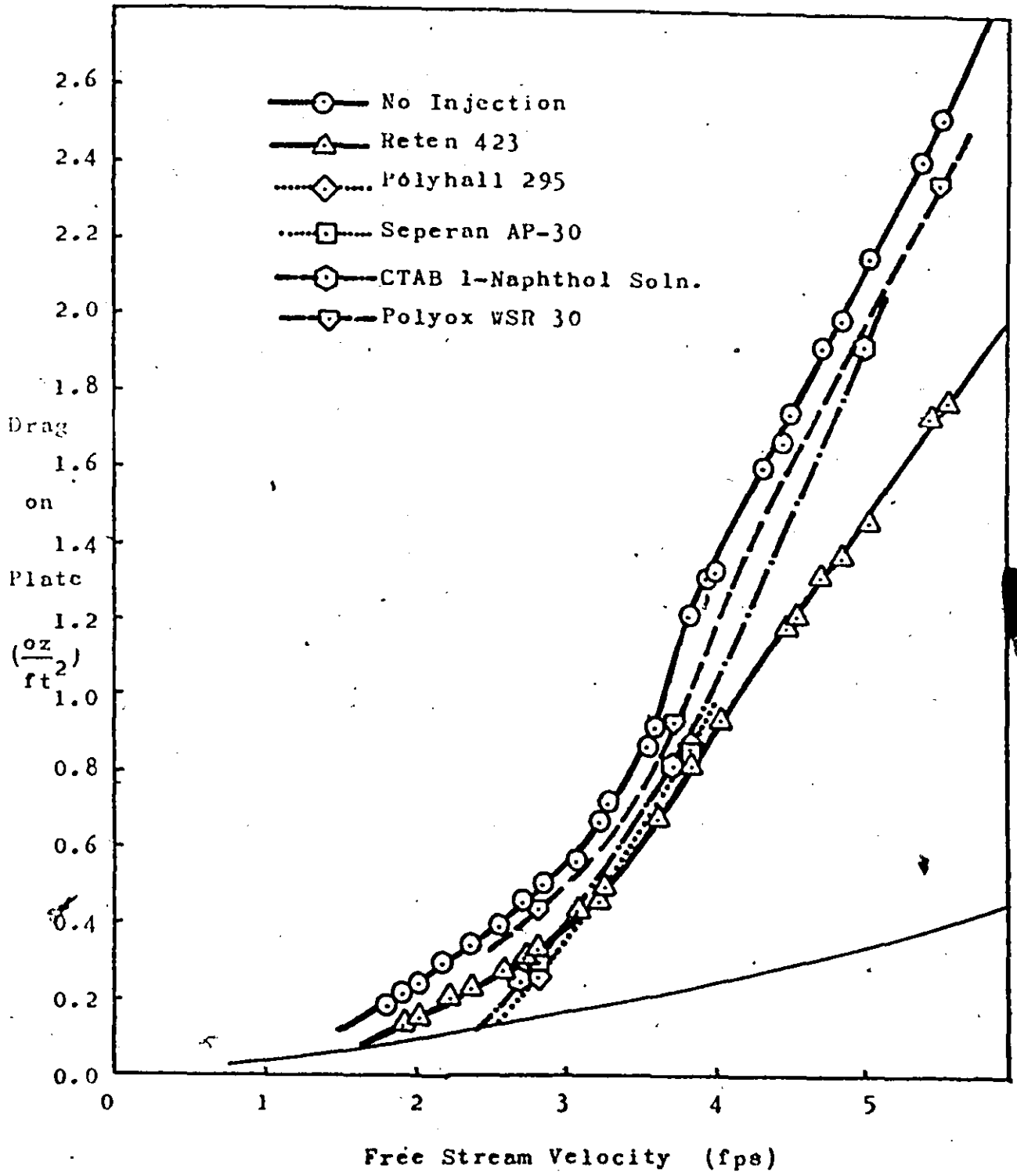

Figure 6.3 Summary of Maximum Drag Reduction Data

Figure 6.3 gives a summary of all the injection data presented in Chapter V. It may be noted that although at lower free stream velocities it is less

effective than the other additives, Reten 423 is more effective at higher free stream velocities. This is probably due to its higher molecular weight, which is of the 10^8 order, whereas Polyhall and Seperan are 10^6.

The CTAB drag reduction is not found to be free stream velocity dependent, but it is expected that at some velocity it will become ineffective because micellar solutions are shear thinning fluids and behave as ordinary Newtonian fluids above a limiting Reynolds number which is dependent on the flow conditions and the micelle concentration, White (9).

The maximum drag reduction, as predicted by Giles in Equation 2.1, is not approached. It is expected however that greater reductions are possible at higher free stream velocities with Reten 423 as the curve with injection in Figure 6.3 is beginning to diverge from the curve with no injection. Additive drag reduction is thought to be based upon some form of turbulence suppression. Since the experimentation was conducted near the Transi - tion Region, due to inadequate free stream velocities, maximal reductions can not be expected.

Figure 6.4 shows percentage drag reduction for Reten 423 as a function of total injection rate and free stream velocity. It may be noted that although higher percentage reductions are attained at U = 1.9 fps than at 5.4 fps, the rate of change of decrease is

decreasing and it is expected that the percentage drag reduction will rise with higher free stream velocities.

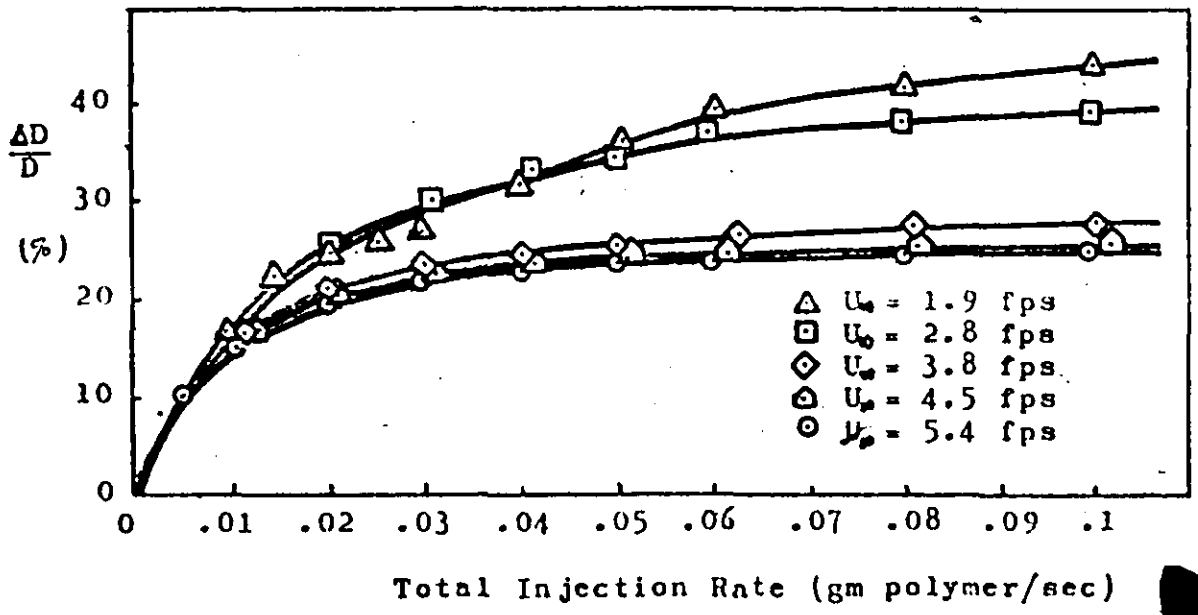

Figure 6.4 Percentage Drag Reduction Curves for Reten 423 as a function of Injection Rate and Free Stream Velocity.

Figure 5.6 indicates that drag reduction may be obtained with aluminum powder present in a flow. The actual mechanism for reduction is not known, but it is expected that the particles of aluminum act similarly to the long chain molecules of the other additives in that they suppress turbulence to some degree.

CHAPTER VII

CONCLUSIONS:

As a summary of the foregoing discussions, the following conclusions can be drawn:

(1) The amount of drag reduction which will occur over a flat plate is dependent upon the concentration of the drag reducing additive present in its vicinity and independent of the concentration or rate of injection of the additive prior to it being found there.

(2) A concentration of 20 wppm seems to be the optimum concentration for maximum drag reduction in both internal and external flows for Retan 423.

(3) One wppm of Retan 423 can produce substantial drag reduction, albeit 50% less than at the optimal concentration of 20 wppm, at the free stream velocities tested. Since this effect is increasing with increasing free stream velocity, it seems that economical employment of additives may be obtained for full size ships.

(4) The composite blotting paper-polymer ablative coatings seem to be very durable and show promise of an even more economical additive employment on a large scale.

(5) Drag reduction was found to be a function of the square of the free stream velocity, as well as the total injection rate. For Reten 423 being

injected into a developing boundary layer over a flat plate (which was 4 ft long and $\frac{1}{2}$ ft wide), the decrease in skin friction drag over its surface may be approximated by;

$$\Delta D = (0.017+0.050_{in})U_\infty^2 \text{ for } .11 \geq 0_{in} \geq 0.02$$

$$\Delta D = (0.01+0.40_{in})\, U_\infty^2 \text{ for } .005 \leq 0_{in} \leq 0.02$$

where 0_{in} = total injection rate of Reten 423 (gm/sec)

U_∞ = free stream velocity (fps) (and should be less than 6 fps).

(6) Immediately after being injected a concentration of additive solution diffuses rapidly but gradually attains a concentration dependent upon both the flow and injection conditions, which diffuses very slowly.

(7) Reten 423, being of higher molecular weight was found to be more effective than the other additives tested in reducing drag, especially with increasing free stream velocity.

(8) Calibration of the velocity meter propeller probe indicates that propeller efficiency is reduced with polymer addition as expected, resulting in a lower frequency of rotation at a given velocity.

CHAPTER VIII

REFERENCES:

(1) Hoyt, J.W., "The Effect of Additives on Fluid Friction," J. Basic Eng., June 1972.

(2) Cadd, G.E., "Friction Reduction," Encyclopedia of Polymer Science and Technology, Vol. 15, Inter. Science., J. Wiley, N.Y., 1971.

(3) Granville, P.S., "The Frictional Resistance and velocity Similarity Laws of Drag-Reducing Polymer Solutions,"NSRDC Report 2502, 1967.

(4) Giles, W.B., "Similarity Laws of Friction-Reduced Flows," Journal of Hydronautics, Vol. 2 1968.

(5) Latto, B., Private communication.

(6) Emerson, A., "Model Experiments Using Dilute Polymer Solutions instead of Water," Trans., N.E. Coast Inst. of Engineers and Shipbuilders, Vol. 81, 1965.

(7) Levy, J., and Davis, S., "Drag Measurements on a Thin Plate in Dilute Polymer Solutions," International shipbuilding Progress, Vol.14,1967.

(8) Latto, B.,and Middleton, J.A."Effect of Dilute Polymer Solutions on External Boundary Layers," Proc. of the Symposium on Turbulence in Liquids, Gordon and Breach,1969.

(9) White, A., Ph.D. Thesis, Middlesex Polytechnic, Council of Nat. Academic Awards, July,1972.

(10) Love, R.H., "The Effect of Ejected Polymers on the Resistance and Wake of a Flat Plate in a Water Flow," Hydronautics Inc.,Tech. Report 353-2,1965.

(11) Kowalski, T.,"Higher Ship Speeds due to Injection of Non-Newtonian Additives," Eastern Canada Section of the Society of Naval Architects and Engineers, Presented in Montreal, January, 1968.

(12) Kilian, F.P., "Verfahren zur Widerstandsverminderung-1,Fortschrittsbericht," Versuchsanstalt fur Wasserbau und Schiffbau,Bericht Nr. 384/67. 1967.

(13) Kim,S., and Tagori.,"Drag Measurements on Flat Plates with Uniform Injection of Polymer Solutions and their Direct Application to the Wall," Proc. Annual Meeting JSME, Oct.1969.

(14) Tulin,M.P. and Wu,J., "Drag Reduction by Ejecting Additive Solutions into Pure-Water Boundary Layer;"Hydronautics, Inc. Tech Report 353-7,1971.

(15) Astarita, G., and Nicodemo,L., "Velocity Distributions and Normal Stresses in Viscoelastic Turbulent Pipe Flows," AIChE Journal, Vol.12, 1971.

(16) Schlichting, H.: "Boundary Layer Theory," McGraw-Hill Book Co. 4th Ed.

(17) "Flow of Fluids Through Valves,Fittings and Pipes," Crane Technical Paper No. 410,1957.

(18) Collins, D.J., "Turbulent Boundary Layer with Slot Injection of Drag Reducing Polymer," Ph.D. Thesis, Georgia Inst. Tech. 1973.

(19) Shen,C.,"An Experimental Study of the Effects of Aqueous Polymer Solutions on a Liquid Boundary Layer," Masters Thesis, McMaster University, Hamilton, 1968.

APPENDIX I

VELOCITY PROBE CALIBRATION:

A 10 foot diameter 2 foot deep tank was constructed which had above it a support system with a 4 foot long arm which could propel the probe concentrically around the tank at linear velocities of up to 20 feet per second. Two photo-sensitive relays were located diametrically opposite each other and enabled accurate time measurement for whole or half revolutions. Some of the measurements were conducted using a two pen plotter, one pen recording the probe output and the other the time interval between relays. Thus, using the plotter timing mechanism, accurate probe velocities were computable and could be compared to the probe signal display. The tank was filled with water and various polymer concentrations.

The calibration chart used for the plate velocity measurements is shown in Figure 10.1. During the course of calibration it was discovered that the position of the calibration curve was very dependent on the adjustment of the fine jewelled bearing which located the propeller axle. If the bearings were too loose the propeller would spin too rapidly and a breakdown of conduction occurred at some velocity resulting in an incorrect reading. If the bearings were tightened until the propeller axle stuck and then backed off slightly the calibration chart would assume the form of Figure 10.1.

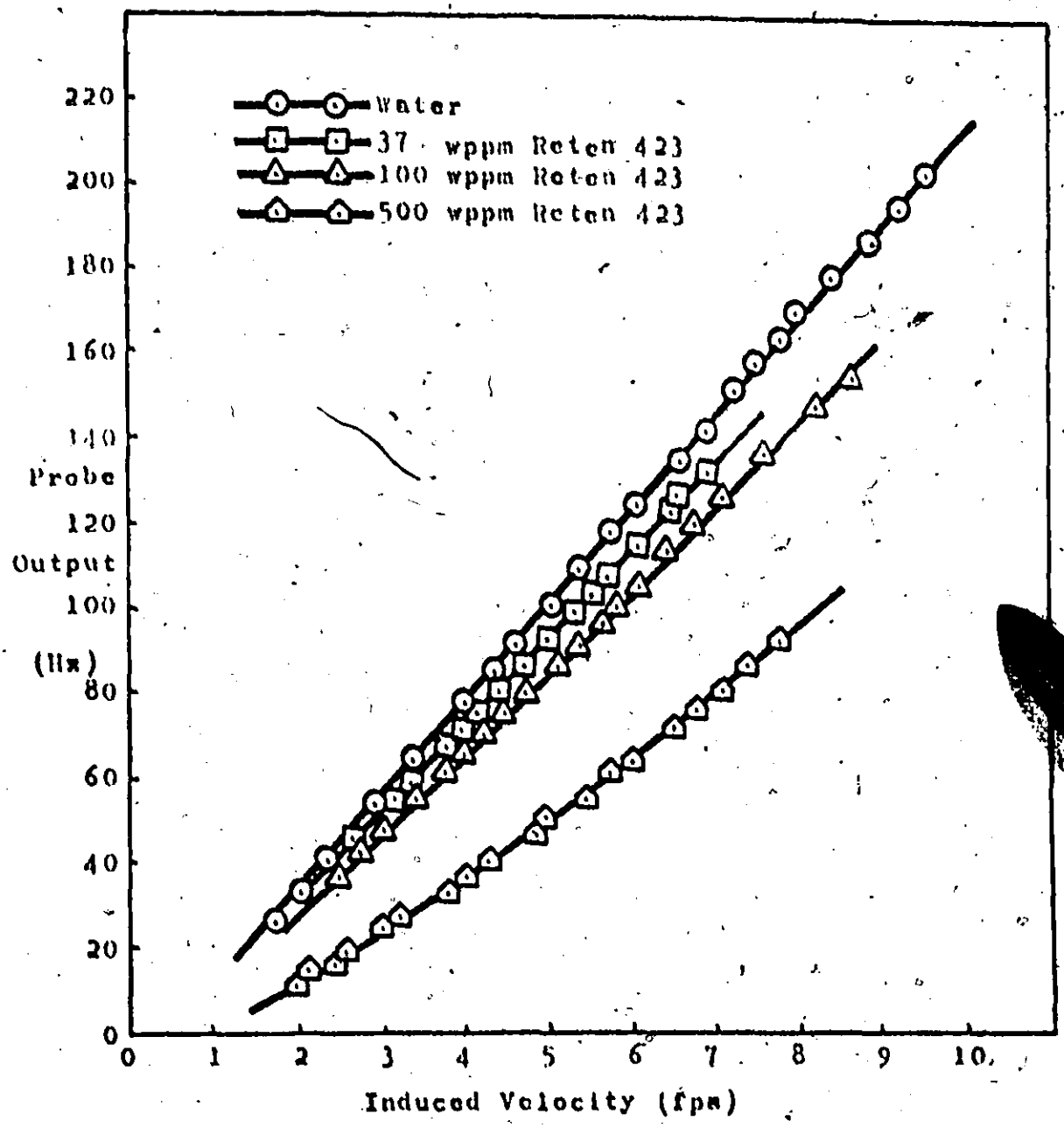

Figure 10.1 Velocity Meter Calibration Chart

After 20 hours of use the probe was found to need bearing re-adjustment as the calibration chart slope was found to decrease. The probes were calibrated before and after any prolonged experimentation period to ensure accuracy.

Figure 10.1 provides calibration for the use of the probe in various polymeric flow conditions. If the con-

centration of the flow can be approximated, or is known, then accurate velocity measurements can be made with relative ease. Problems, such as those encountered with pitot-probes and hot wire anemometers measuring polymeric flows due to molecular entanglements about the probes and different heat transfer rates, are overcome using this type of probe. Calibrations of concentrations less then 20 wppm proved almost indistinguishable from those of water making this instrument ideal for measuring velocity profiles in the boundary layer over a flat plate experiencing a polymeric injection since concentrations greater than 20 wppm are seldom encountered there.

The main drawback of this type of instrument is that it has a relatively large size, the propeller being .3 inches in diameter, Thus, velocity readings must be averaged over the probe area and finer differentiations are not directly possible. It is possible, however, to traverse in very fine steps taking many average velocity readings, and produce reasonably accurate profiles.

APPENDIX II

MOMENTUM THICKNESS ANALYSIS:

Estimation of the drag distribution over the flat plate was attempted by taking a number of velocity profiles during an injection. The total drag obtained from this analysis should also confirm that obtained by the direct measurement procedure.

11.1 Theoretical Development of Drag Measurement Using a Velocity Profile:

Momentum thickness is defined as;

$$\delta_2 = \int_0^{\infty} \frac{u}{U_\infty}\left(1-\frac{u}{U_\infty}\right) dy \qquad (11.1)$$

where all the quantities are defined in figure 11.1. Normalizing both axes, yields figure 11.2 and equation 11.2, which is

$$\delta_2 = \delta \int_0^1 \frac{u}{U_\infty}\left(1-\frac{u}{U_\infty}\right) d\eta \quad \text{where } \eta = \frac{y}{\delta} \qquad (11.2)$$

where δ = boundary layer thickness

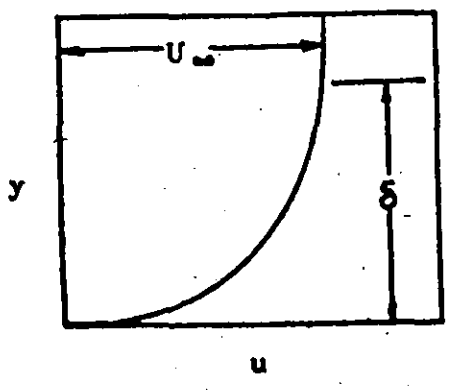

Figure 11.1 Velocity Profile

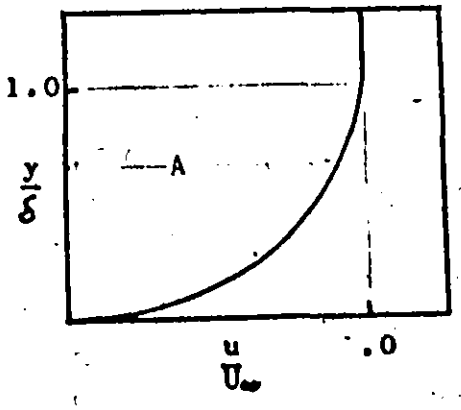

Figure 11.2 Normalized Velocity Profile

From Figure 11.2 it may be seen that

$$A = \frac{u}{U_\infty}$$

Expanding Equation 11.2 results in Equation 11.3.

$$\frac{\delta}{\delta}_2 = \int_0^1 \frac{u}{U_\infty} d\eta - \int_0^1 \left(\frac{u}{U_\infty}\right)^2 d\eta \qquad (11.3)$$

$\int_0^1 \frac{u}{U_\infty} d\eta$ may be obtained by computing the area designated by A in Figure 11.2. $\int_0^1 \left(\frac{u}{U_\infty}\right)^2 d\eta$ may be obtained similarly by plotting values of $\left(\frac{u}{U_\infty}\right)^2$ against $\frac{y}{\delta}$ in Figure 11.2 and then computing the corresponding area. Subtracting the two areas from each other and multiplying the result by δ, results in a value for δ_2. (δ is obtained by noting the distance at which U_∞ occurs nearest the plate.) Plotting the values of δ_2 so obtained at various positions along a flat plate results in Figure 11.3.

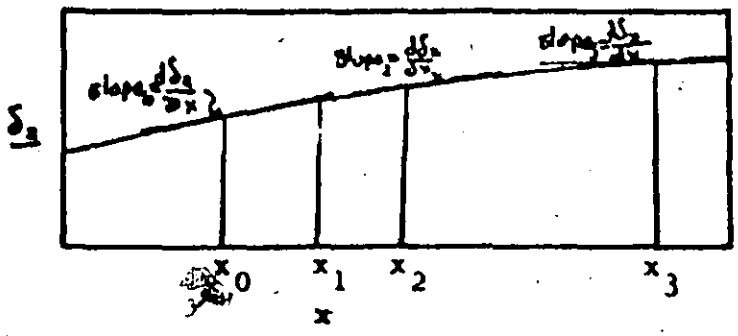

Figure 11.3 Momentum Thickness along the Length of a Flat Plate.

Wall Shear Stress may be defined as

$$\tau_o = \rho U_\infty^2 \frac{d\delta_2}{dx}, \qquad (11.4)$$

and since the drag on the plate may be defined as

$$D = w \int_0^L \tau_o \, dx \quad \text{where } w = \text{plate width} \qquad (11.5)$$

the drag on the plate may be computed by

$$D = w\int_{x_0}^{x_L} U_\infty^2 \rho \frac{d\delta_2}{dx}dx$$

$$= w\rho U_\infty^2 \int_{x_0}^{x_L} \frac{d\delta_2}{dx}dx. \qquad (11.6)$$

If the slopes of the curve are taken from Figure 11.3 and plotted against x as shown in Figure 11.4, $\int_{x_0}^{x_L}\frac{d\delta_2}{dx}dx$ may be obtained by taking the area under the curve so obtained.

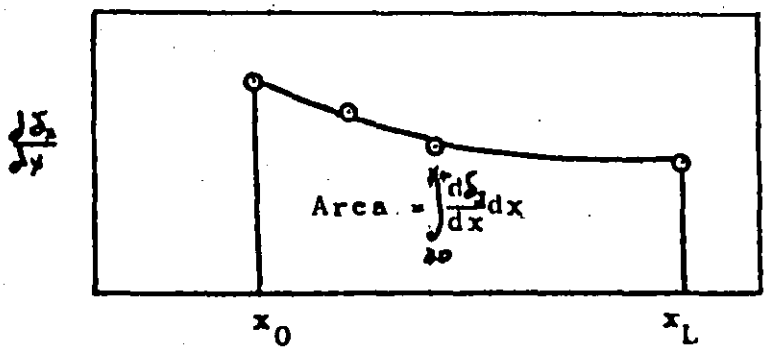

Figure 11.4 Determination of $\frac{d\delta_2}{dx}dx$ from a plot $\frac{d\delta_2}{dx}$ vs x.

11.2 Drag Approximation using Experimental Velocity Profiles:

Four velocity profiles were taken in a flow over the flat plate at a stream velocity of 4.15 fps and, at the same locations, during a 50 ml/sec injection of 1000 wppm concentration of Reten 423. The profiles were taken at the leading edge of the test section and 1, 2, and 4 feet downstream of it. Figure 11.5 presents the normalized data for flow without injection and Figure 11.6, the data with injection.

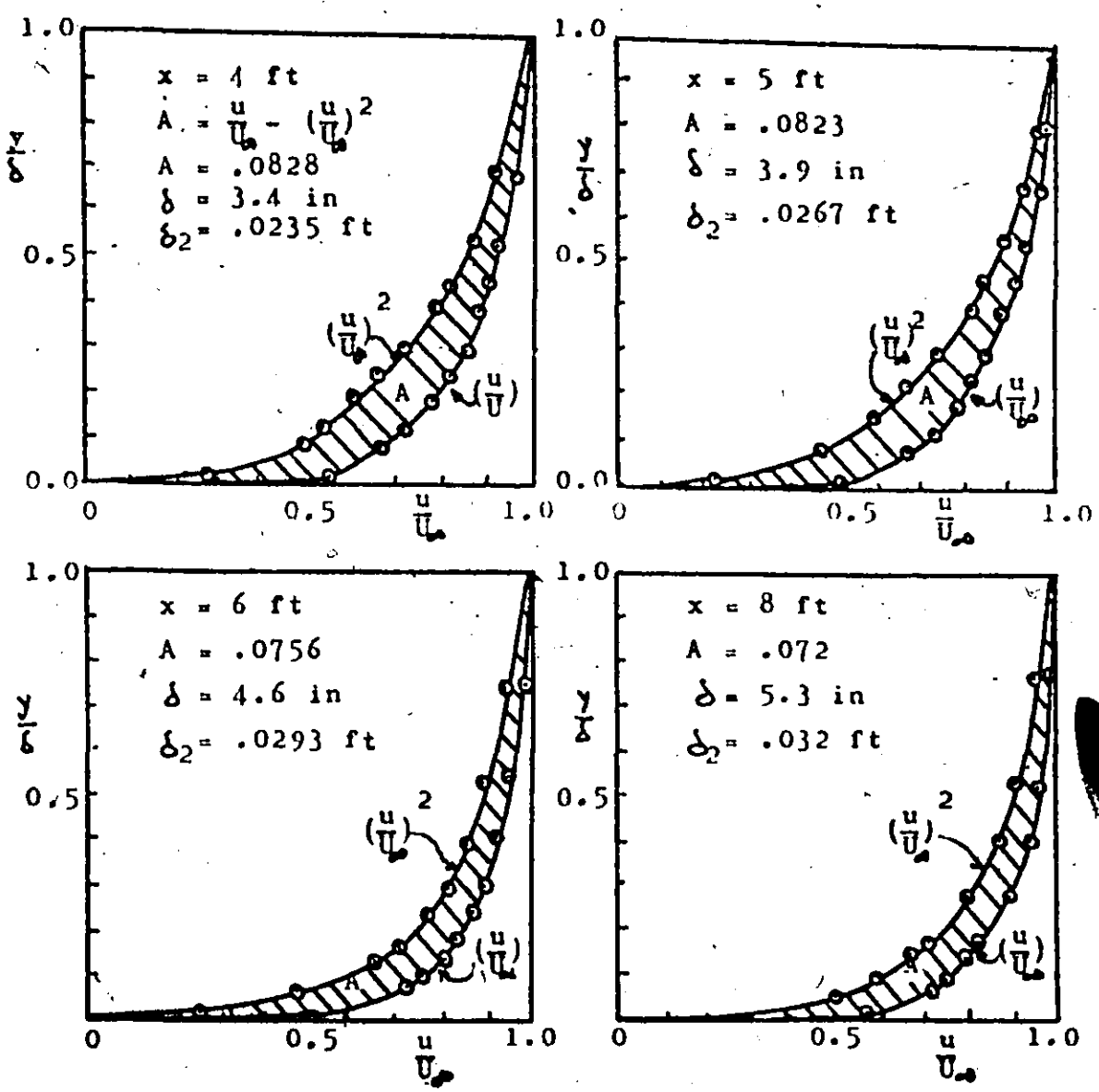

Fig.11.5 Velocity profiles over test section at U = 4.15 fps with no injection.

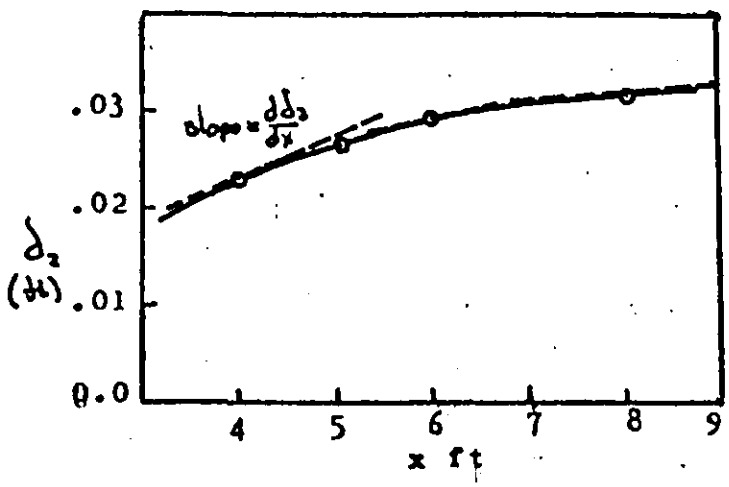

Fig. 11.6 δ_2 versus x.

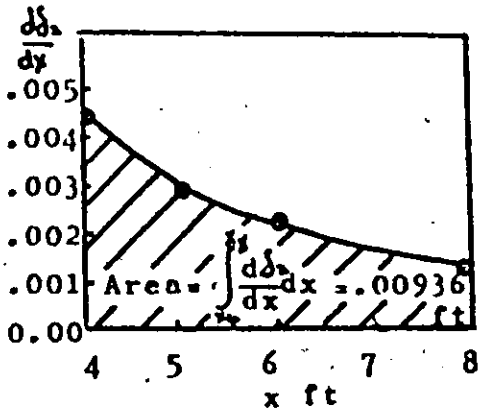

Fig. 11.7 Determinntion of $\int_{x_0}^{x} \frac{d\delta_2}{dx} dx$

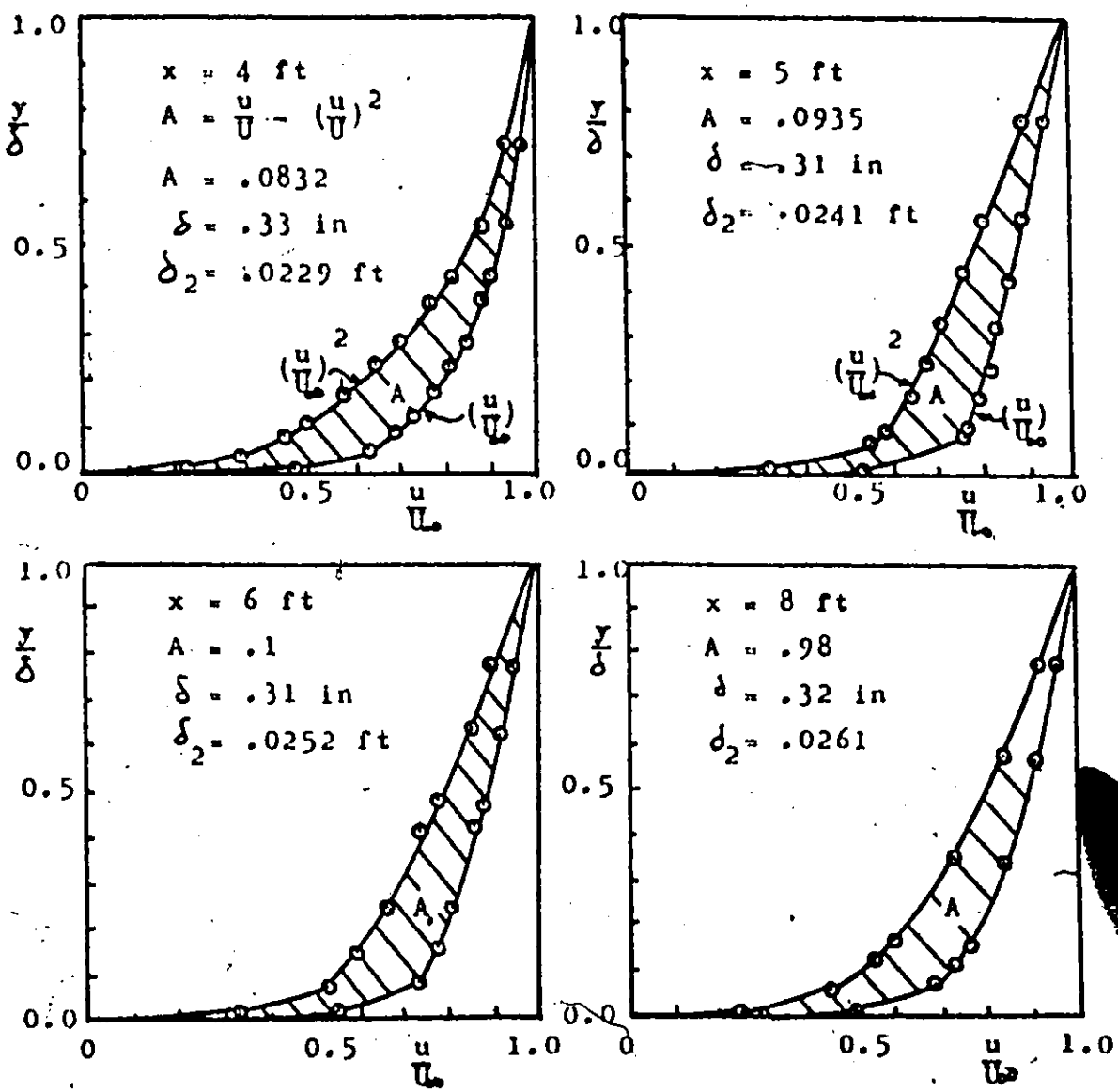

Figure 11.8 Velocity Profiles over Test Section at U_∞=4.15 fps with injection of 1000 wppm Reten 423 at 50 ml/sec.

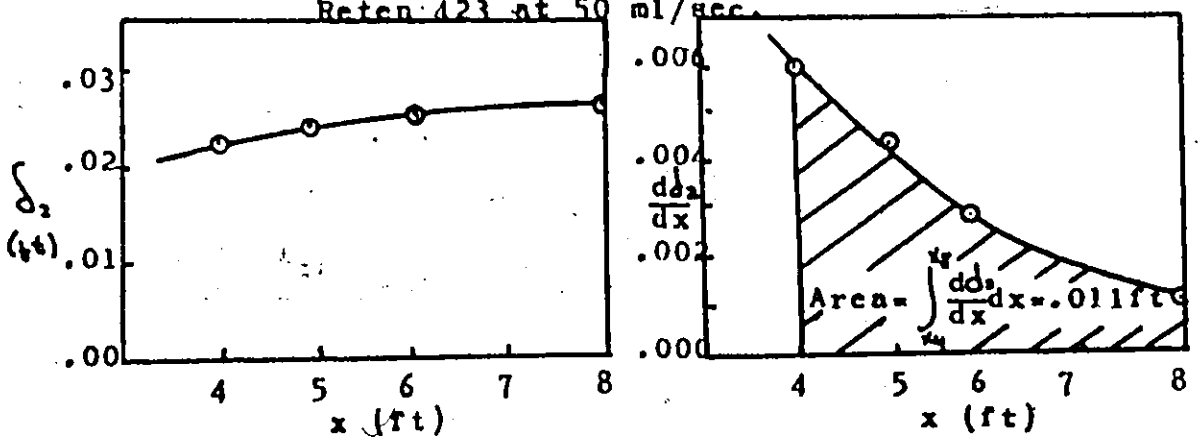

Figure 11.9 Momentum Thickness against distance along test section.

Figure 11.10 Determination of $\int_{x_1}^{x_2} \frac{d\delta_2}{dx} dx$

Figure 11.6 plots δ_2 versus x such that the slope of the curve may be measured and plotted in Figure 11.7 as $\frac{d\delta_2}{dx}$ vs x. The area under the curve in Figure 11.7 yields $\int_{x_1}^{x_2} \frac{d\delta_2}{dx} dx = .00936$ ft. The total drag on the plate is now obtained using equation 11.6, that is;

$$D = w\rho U_\infty^2 \int_{x_1}^{x_2} \frac{d\delta_2}{dx} dx$$

$$= \frac{62.4}{32.2}(4.15)^2 (.00936)$$

$$= .156 \text{ lb}_f/\text{ft}^2$$

$$= 1.25 \text{ oz}_f/\text{ft}^2$$

This result compares to 1.45 oz_f/ft^2, as obtained by direct measurement. The discrepency is due to averaging the velocities over the probe area and not having enough sample velocity profiles.

Figures 11.8, 11.9 and 11.10 correspond to 11.5, 11.6 and 11.7 respectively but for flow with an injection of 1000 wppm Reten 423 at 50 ml/sec. A similar analysis yields 1.48 oz_f/ft^2 for drag over the test section for this condition. The measured drag for this test condition is found to be 1.2 oz/ft^2 from Figure 5.2b. Other researchers have noted a similar discrepancy using momentum thickness analyses for drag prediction. Collins(18) noted the decrease in boundary layer thickness with polymer injection yet drag reduction was not evident from analysis. Shen (19) did not obtain evidence of drag reduction with injected polymer solutions in some of his tests from momentum

theorem analyses. In the present work, "fuller" velocity profiles were obtained for flow over the flat plate experiencing injection than for the case of no injection. This implies that, since less drag is expected from "fuller" velocity profiles, as the body producing the drag has less influence in disturbing the free stream than a body in a situation with a less full velocity profile, the results of the momentum analysis should have indicated less drag for the fuller velocity profiles, obtained from the flow with polymer addition. This may indicate that the determination of δ may be erroneous or that more precise velocity profiles are necessary.

It is suggested however, that momentum thickness analyses may not be appropriate for estimating drag if polymers are present in the flow.

APPENDIX III

APPROXIMATION OF INJECTED POLYMER CONCENTRATION IN BOUNDARY LAYER:

This method assumes that complete dilution occurs within the boundary layer. That is, if a boundary layer flowrate of 3000 ml/sec is occurring and a 2000 wppm polymer concentration is introduced at a rate of 30 ml/sec, a uniform concentration of 20 wppm will result. Although there is no reason for the injection to remain within the boundary layer and although concentration gradients are known to exist this type of approximation will give some insight into the quantity of polymer required within the boundary layer to produce the measured drag effects presented in Chapter V.

The boundary layer flowrate will be simply approximated by equation 12.1.

Q_{bl} = (Average boundary layer velocity)(Average boundary layer thickness over the plate)(width of the plate) (12.1)

The average boundary layer velocity, based upon the velocity profiles taken, was assumed to be 0.9 U_∞.

The boundary layer will be assumed fully turbulent and the average thickness will be approximated by taking half the sum of the leading and trailing edge thicknesses as predicted by equation 12.2, which may be found in any fluid mechanics text.

$$\frac{\delta}{x} = 0.379/(Re_x)^{1/5} \qquad (12.2)$$

Figure 12.1 lists the flowrates obtained by this method over a number of free stream velocities.

U_{∞} (fps)	5.4	4.5	3.8	2.8	1.9
Q_{bl} (ml/sec)	7950	7000	5950	3960	3000

Figure 12.1 Boundary layer flowrate approximation

Lines of constant concentration may now be plotted on Figure 6.1. A flowrate of 3000 ml/sec requires 60,000 wppm-ml/sec to be introduced into it for a concentration of 20 wppm to result. Thus Figure 12.2 is obtaied by noting that .01 gm polymer = 10,000 wppm.

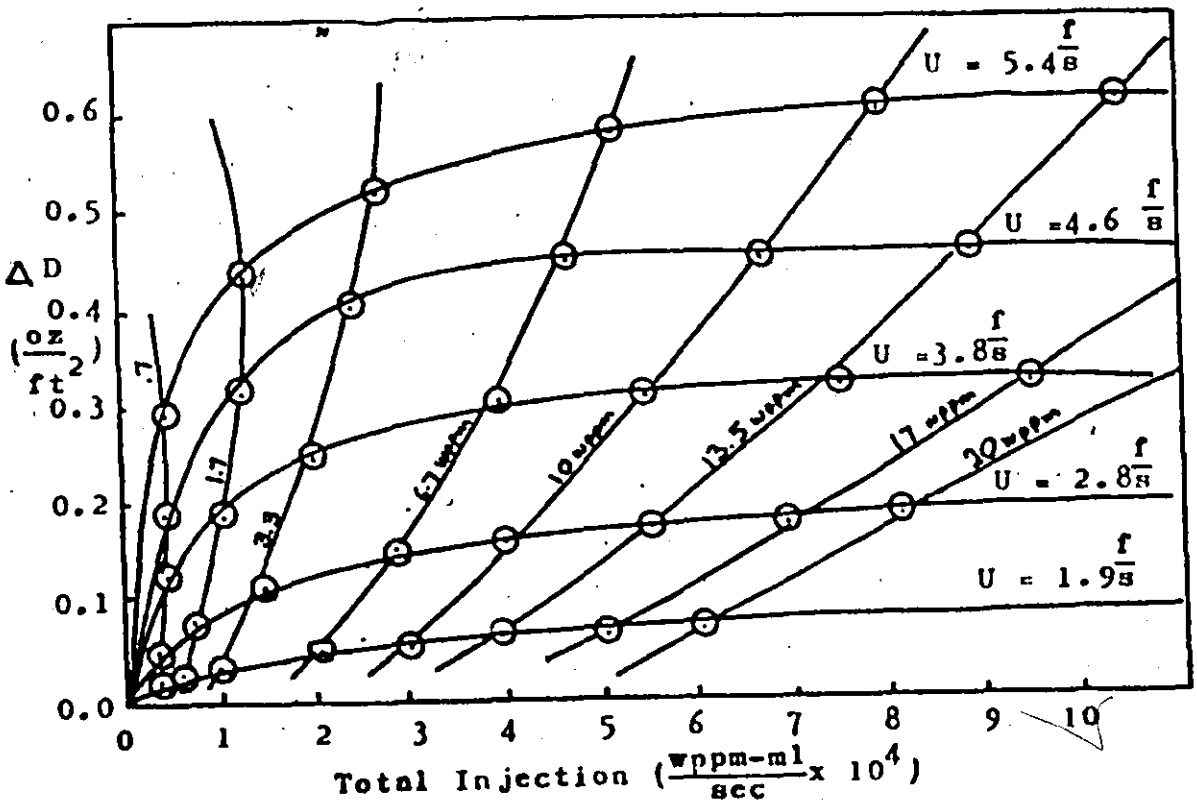

Figure 12.2 Lines of Constant Concentration plotted against the Drag Reduction Data of Figure 6.1

APPENDIX IV

PHOTOGRAPHIC STUDY OF INJECTED POLYMER CONCENTRATION:

Photographs such as that shown in Figure 13.1 were used to obtain Figures 13.2 and 13.3. The visible extent of the dye was traced onto a known scale and measurements were taken from the photographs by comparing the distances involved. As may be seen the injection rate does not seem to have a predictable effect on the size of the injection envelope. This may be explained by the dye diffusing beyond perception, although care was taken to include equal amounts of dye for each injection.

The concentration of the injected polymer was 500 wppm and Figure 13.2 shows the injection envelopes for a free stream velocity of 2 fps while Figure 13.3, that for 5.4 fps.

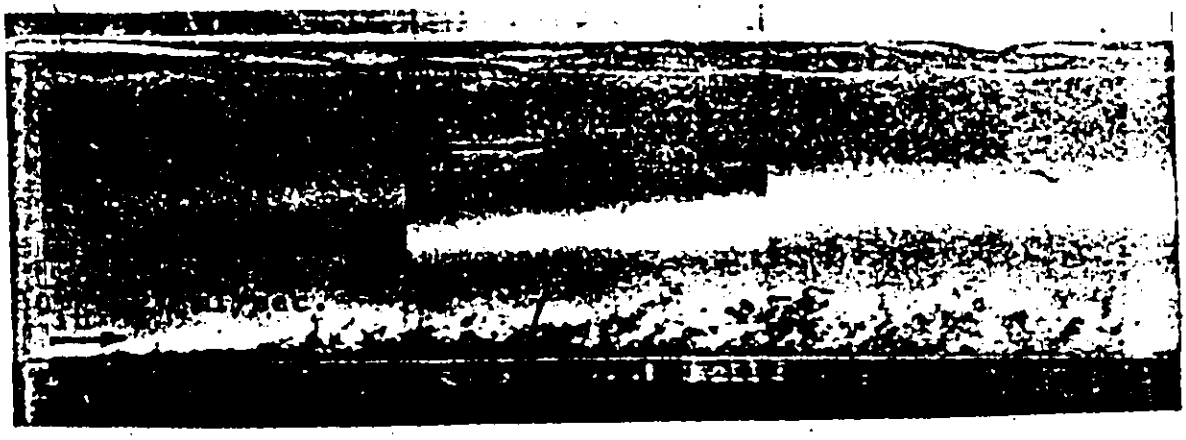

Figure 13.1 Photograph of 500 wppm Reten 423 Injection Into a 2 fps Free stream at 27 ml/sec.

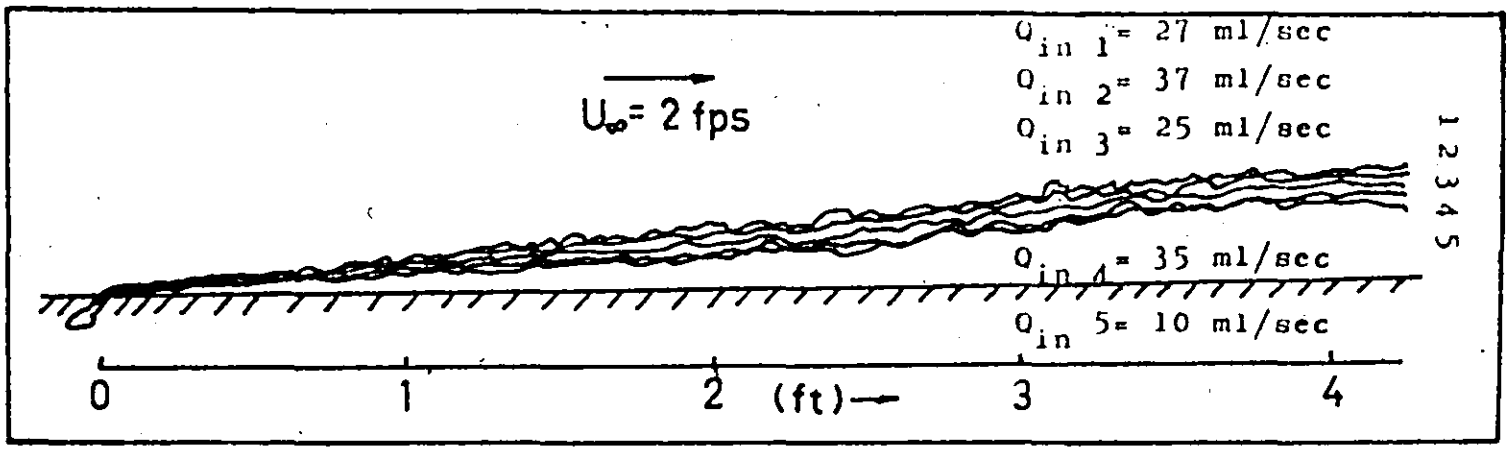

Figure 13.2 Injection Profiles at U_∞ = 2 fps for Various Injection Rates of 500 wppm Retan 423.

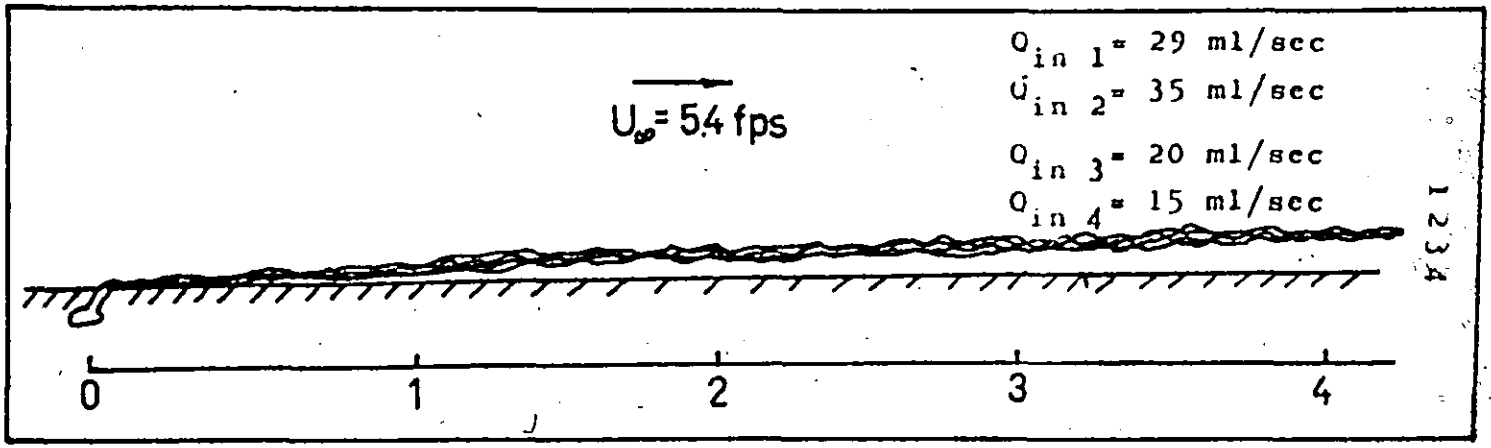

Figure 13.3 Injection profiles at U_∞ = 5.4 fps

Figure 13.4 may now be drawn using the mid point of each cluster of injection envelopes as a datum . Information was obtained for flows of 2 and 5.4 fps only. As the intermediate injection thicknesses are unknown a linear relationship will be assumed but drawn using a broken line.

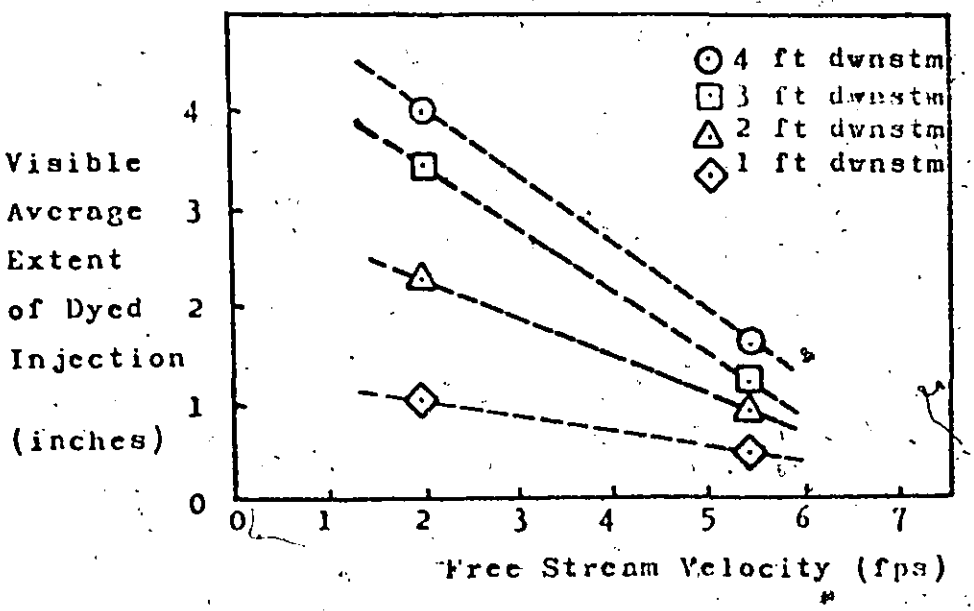

Figure 13.4 Summary of Injection Envelope Thicknesses

It is obvious that the linear relationship is incorrect as it insinuates no thickness at some U_∞.

Assuming uniform diffusion and U in the region near the wall about .9 U_∞ and a 50 ml/sec injection rate, Figure 13.5 may be drawn.

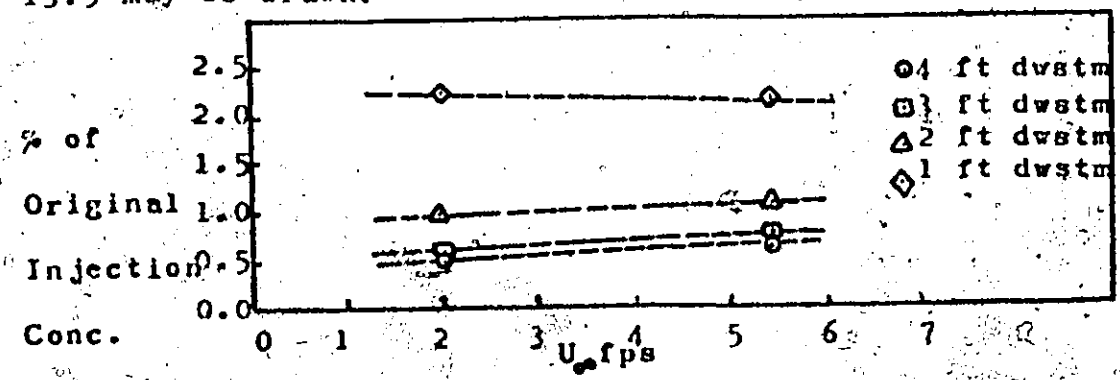

Figure 13.5 Percent of Injection Concentration at Various Positions assuming 50 ml/sec Injection Rate.

The percentage of the original concentration is obtained by dividing the injection flowrate by the flowrate from Figure 13.4 at each of the indicated positions. The flowrate is obtained by multiplying the injection cross sectional area by the assumed $.9U_\infty$ near the wall.

It is now possible to predict what the concentration is over the plate. Consider a 500 wppm concentration being injected at 50 ml/sec. This yields a total injection rate of 25,000 wppm-ml/sec. If the free stream velocity is 2 fps, Figure 13.5 predicts that 0.5% of the original injection concentration which is 2.5 wppm, should be found 4 feet downstream. At U = 2 fps, Figure 12.2 predicts a uniform concentration of 8.5 wppm. If the concentrations are determined for the other positions along the plate an average concentration of about 8 wppm is obtained.

Figures 13.4 and 13.5 are rather crude but they provide reasonable information and it is suggested that the method shown here could be very useful and rigorous if Figure 13.4 were obtained in more detail.

Figure 13.6 shows the predicted concentrations over a plate with 500 wppm injection into U = 2 fps.

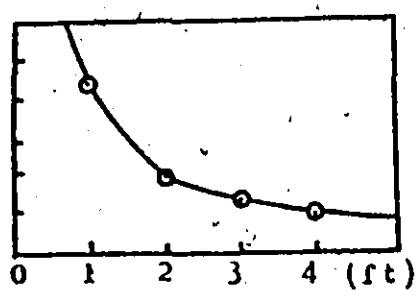

Figure 13.6 Estimated Concentration resulting from injecting 500 wppm Retan into a free stream of 2 fps at 50 ml/sec.

APPENDIX V

INVESTIGATION OF RETAN 423 EFFECTIVENESS IN INTERNAL FLOW CONDITIONS:

14.1 Description of Apparatus:

A simple rheometer, which produced turbulent flow in a tube, was used to measure the average skin friction coefficient for a number of Retan 423 concentrations. The rheometer consists of a simple volume calibrated reservoir which can be pressurized to 30 psi guage pressure by means of a regulated compressed air supply working through a low pressure precision regulator. A length of known diameter stainless steel capillary tubing is attached to the bottom of the reservoir. A straight through valve, mounted at the end of the capillary, allows on-off flow control.

14.2 Theoretical Considerations:

Consider level(1) to be the top level of the fluid in the reservoir and level(2) to be the bottom of the capillary tube. For this arrangement Bernoulli's equation may be written as,

$$\frac{P_1}{\rho} + \frac{V_1^2}{2g} + H_1 = \frac{P_2}{\rho} + \frac{V_2^2}{2g} + H_2 + \frac{kV_2^2}{2g} + \frac{2C_f V_2^2 L}{Dg}$$

where $\frac{kV_1^2}{2g}$ is the head loss at the inlet of the tube and C_f is the friction factor defined as $(\frac{\tau_o}{\frac{1}{2}\rho V_2^2})$. Since the datum line can be placed at level (2), H_2 is zero. Because the diameter of the

reservoir is large compared to the that for the capillary, V_1 is negligible. The velocity in the tube V_2 is calculated from the total volume passed, the cross sectional area of the capillary and the time interval required for passage. Let $V_2=V$, thus,

$$\Delta p = (p_1 + \rho g H_1 - p_2),$$

and Bernoulli's equation may be rewritten as

$$\Delta p = (1+k)\frac{\rho V^2}{2g} + \frac{C_f V^2 L}{Dg}$$

$$\text{or} \quad C_f = \left(\Delta p - (1+k)\frac{\rho V^2}{2g}\right)\frac{Dg}{2\rho L V^2}.$$

The value of k which is the factor for inlet losses is taken as 0.78 (17), while Δp for the experiment is evaluated from the following equation;

$$\Delta p = (p_g + P_{atm} + P_c) + \rho g H_1 - P_{atm}$$

where p_g = guage pressure

P_{atm} = atmospheric pressure

P_c = correction for pressure guage

H_1 = height of fluid above the exit end of the tube

Bernoulli's equation can be applied to both laminar and turbulent flow conditions and the above expression for C_f can be used over a range of Reynolds numbers.

The computer program included at the end of this Appendix was used to calculate the values of C_f and Reynolds number which are plotted in Figure 14.1 for over a range of polymer solution concentrations.

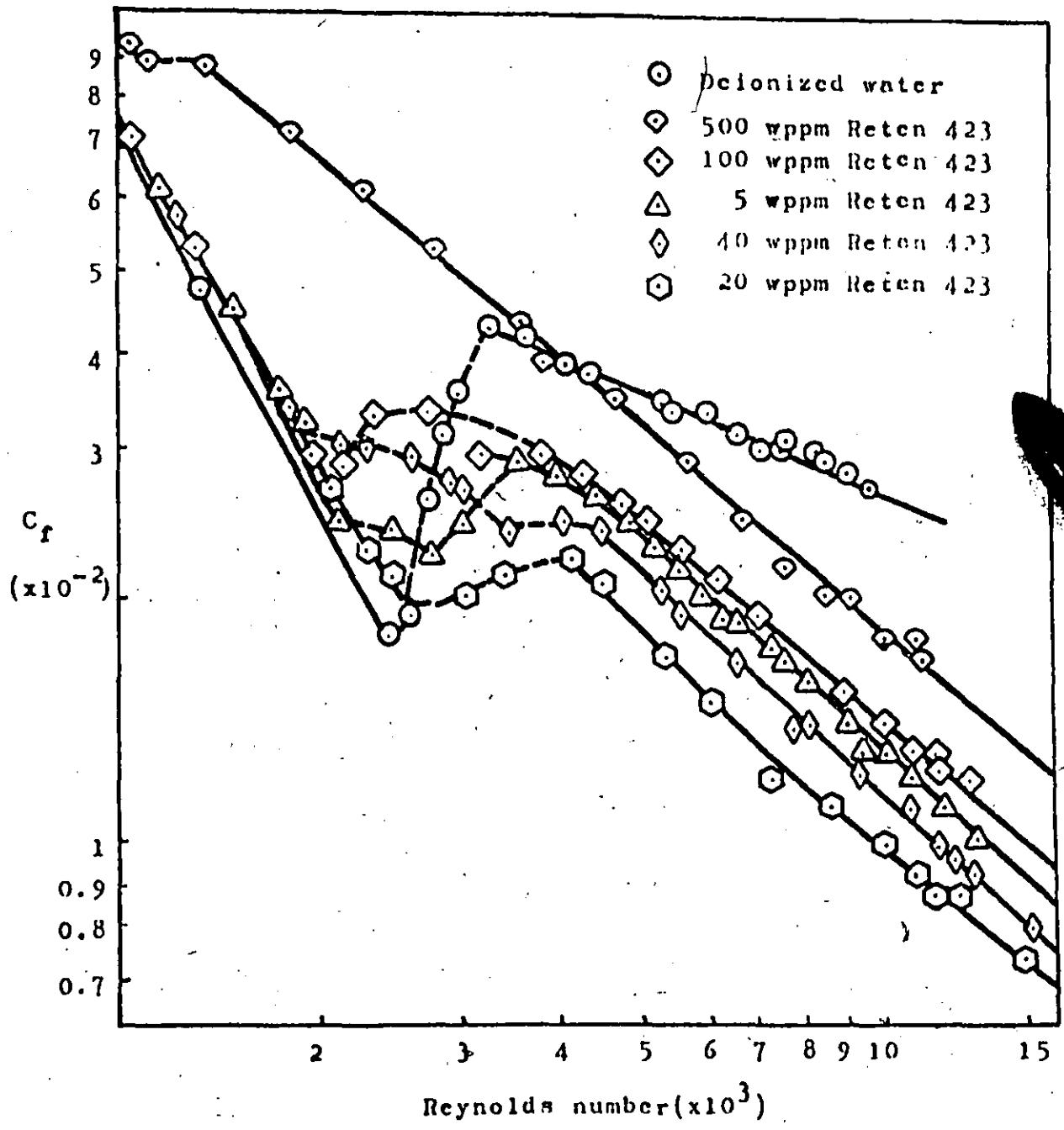

Figure 14.1 Friction Factor- Reynolds number corelation for various concentrations of Reten 423.

14.3 Discussion:

It may be noted that maximum reduction of C_f occurs, in Figure 14.1, for a concentration of 20 wppm. This indicates that concentrations below this are too dilute while concentrations above become more viscous to the point that increased viscous drag outweighs any additional drag reduction.

Figure 6.2 shows an approximated concentration effectiveness relationship for Reten 423. It is interesting to note that 20 wppm is being approached as a maximum drag asymptote. Although none of the injected flows exceeded a 20 wppm concentration in the boundary layer over the flat plate it is expected that concentrations in excess of 20 wppm would show a definite decrease in drag effectiveness.

APPENDIX VI

CONCENTRATION PREDICTION BY VISCOSITY MEASUREMENT:

During the ablative coating experiment six samples were collected at various points over the test section as shown in Figure 15.1. A pitot probe was positioned at the required site, suction was applied to draw the sample through a tube attached to the probe and a quantity of the fluid was allowed to collect in a test tube. This procedure was repeated at the other sites and then the viscosities of the samples were taken at 20 and 28 degrees C using a Brookfield cup and cone viscometer. The results are shown in Figure 15.2 and plotted against the viscosities of known concentrations in Figure 15.3.

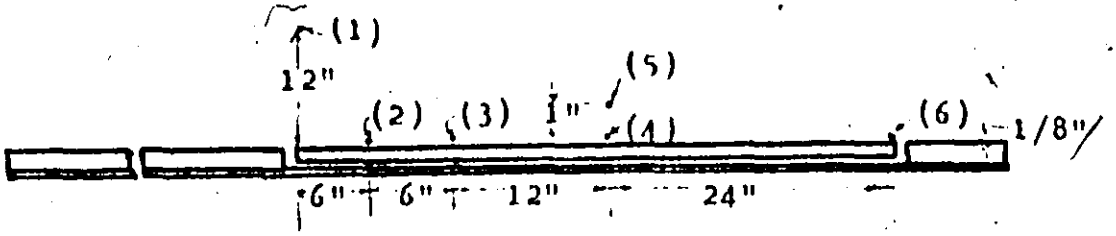

Figure 15.1 Location of Sampling Sites

Site no.	1	2	3	4	5	6
Viscosity @ 20°C (cps)	1.121	1.215	1.211	1.17	1.165	1.14
Viscosity @ 28°C (cps)	.914	.994	.97	.95	.94	.93

Figure 15.2 Viscosity Data as collected over Ablative Surface.

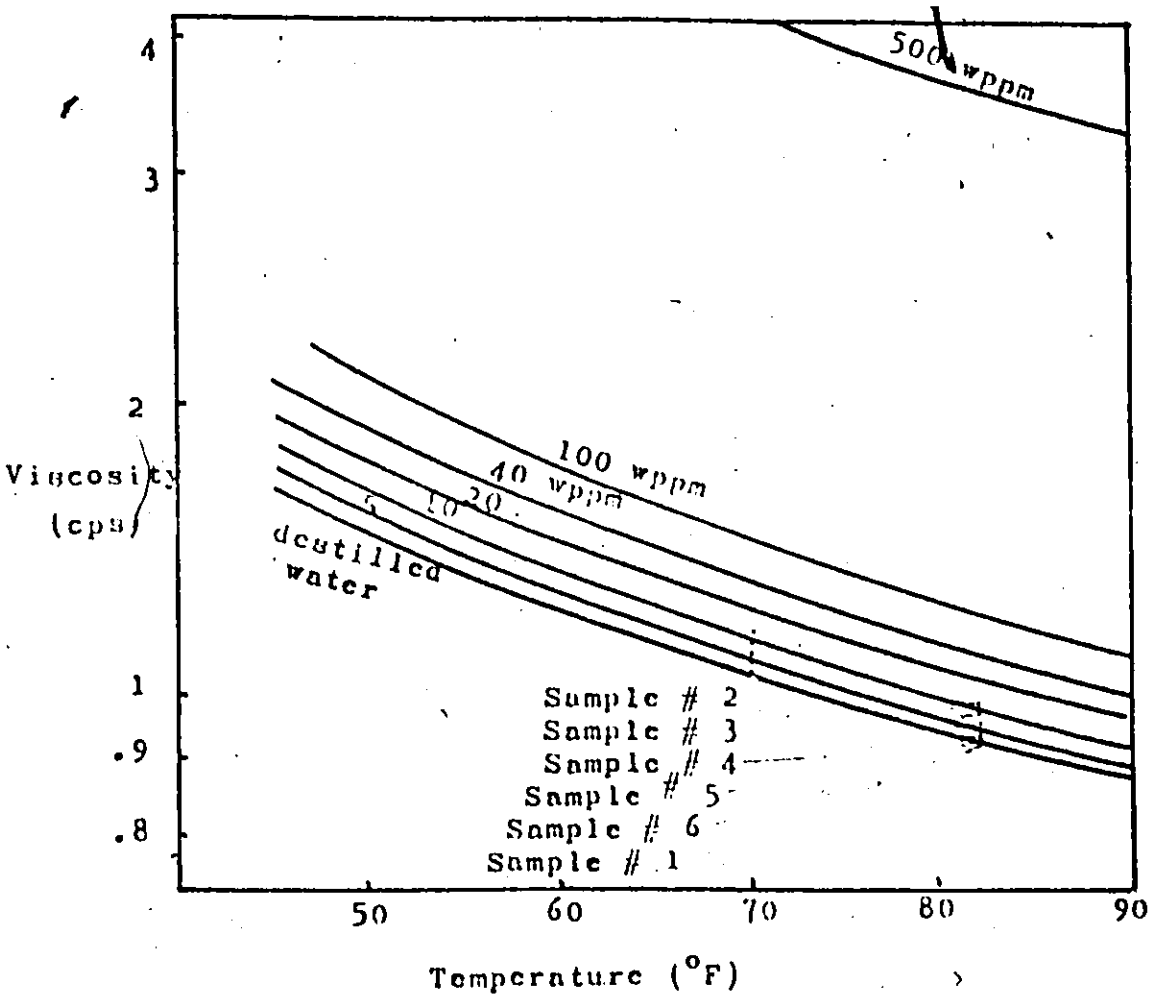

Figure 15.3 Viscosity data for Reten 423, showing samples taken over ablative coating compared to known concentration viscosities.

It is not known whether degradation occurs as a result of the ablative coating technique of polymer addition or how much degradation takes place within the flow. It is not possible to test the samples for drag reduction effectiveness, as much larger sample sizes would be required. The concentration distribution illustrated in Figure 15.4 seems reasonable if the amount of drag reduction obtained with the ablative coating is considered.

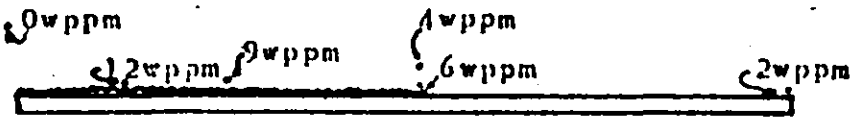

Figure 15.4 Approximate concentration distribution above test section with ablative coating mounted, based upon viscosity comparison.

Since there is evidence that the polymeric effectiveness decreases with degradation, accurate sampling of effective concentration is important. However, degradation may produce a viscosity which is not indicative of true concentration.

If degradation studies indicate that viscosity is indicative of the drag reduction effectiveness of a polymer concentration or if no degradation can be insured, then this method of determining concentrations may be very useful due to its simplicity.